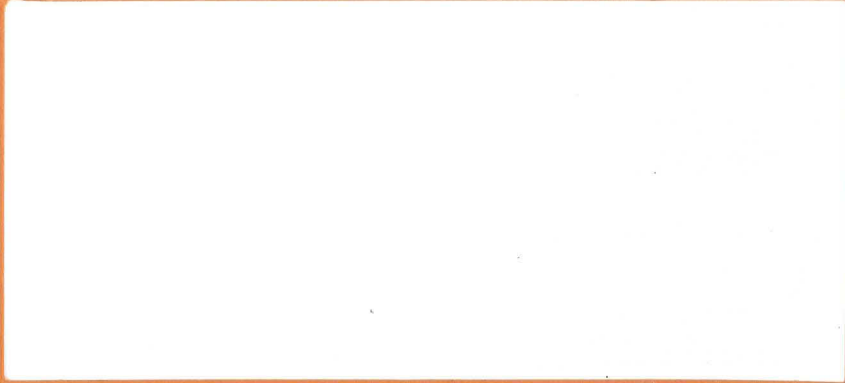


UNITED NUCLEAR  
CORPORATION  
OFFICE COPY  
RETURN TO  
GALLUP OFFICE



7/80



SCIENCE APPLICATIONS, INC.

NATURAL RESOURCES DIVISION

GEOLOGY OF THE CHURCH ROCK AREA, NEW MEXICO

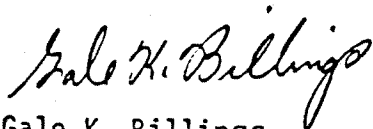
31 July 1980

Mr. Thomas Hill  
Director of Tailings Management  
United Nuclear Corporation  
Mining and Milling  
4801 Indian School Road, N.E.  
Albuquerque, New Mexico 87110

Dear Mr. Hill:

Enclosed is the report concerning geology of the Church Rock area and the UNC mill site. This is the most extensive geologic study of any mill site of which I am aware. It was carried out under the direction and active participation of Dr. John Gibbons of Bearpaw Geosciences, an SAI consultant.

Sincerely,



Gale K. Billings  
Vice President

GKB/kh

Enclosure

GEOLOGY OF THE CHURCH ROCK AREA, NEW MEXICO

for

UNC MINING AND MILLING

by

SCIENCE APPLICATIONS, INC.  
NATURAL RESOURCES DIVISION

and

BEARPAW GEOSCIENCES

## EXECUTIVE SUMMARY

The main part of this study addresses the distribution and geometry of natural rock fractures in the area of the tailings ponds at the Church Rock site. The definition of rock fracturing is necessary to the geo-hydrologic modeling of groundwater and possible seepage movement through the rocks. Two families of fractures are present in the Gallup and Dilco Sandstones which are in the pond area.

The most widespread family of fractures is composed of vertical fractures which strike northeast and northwest in what is often called a regional orthogonal fracture pattern. These fractures are the result of the load imposed by burial and high hydrostatic pressures when the sediments were young. These fractures exhibit a wide average spacing of one fracture per ten feet and tend to be interconnected.

The second family of fractures is the result of monoclinial folding related to ancient basement faults which do not penetrate to the present surface. These fractures are distributed in linear zones which follow the trends of the folds and are locally very dense. These local fracture patterns occur only at the surface; however, this type of pattern penetrates deeply into the subsurface. Two fracture zones of this type pass through the pond area and a third passes nearby. Vertical migration of seepage would tend to be contained within the sandstone fractures because they do not continue through the underlying shales into the next sandstone unit.

## TABLE OF CONTENTS

	<u>Page</u>
Executive Summary	i
TABLES	iii
FIGURES	iv
PLATES	v
Geology of the Church Rock Site	1
Introduction	1
Stratigraphy and Depositional History	1
Regional Tectonics	9
Local Structural Geology	12
Introduction	12
Approach	12
Structural Geology of the Site Region	15
Structural Geology of the Site	17
Structural-Depositional History	18
Monoclinal Folding	18
Age of Monoclinal Folding	24
Fracture Patterns	27
Introduction	27
Extent of Local Fracture Patterns at the Site	27
Regional Fracture Pattern	27
Fracture Zones Associated with Monoclines	31
Distribution of Regional Fracture Patterns	32
Sowers Calculation	33
Relationship of Fracture Spacing to Rock Type and Bed Thickness	37
Relationship of Photolines to Fracture Patterns	40
Summary	40
Hydrogeologic Impact	42
Seismotectonics	44
Introduction	44
Regional Tectonic History: Summary	45

	<u>Page</u>
Seismic Potential of Faults in the Site Region	45
The Pipeline Canyon Lineament	45
Seismic History of the Region	47
Appendix A: Fracture Study Analysis	50
Appendix B: Aerial Photograph Lineament Analysis	85
References Cited	96

## TABLES

	<u>Page</u>
TABLE I. Summary of Stratigraphic Units and Lithology, Pipeline Canyon Area	3

## FIGURES

<u>Figure</u>	<u>Page</u>
1. Generalized geologic section.	6
2. Colorado Plateau plate tectonic subprovince.	10
3. ERTS imagery aerial photograph.	13
4. Pinedale monocline.	16
5. Sand dike.	19
6. Sand boil.	20
7. Sand dike.	21
8. High pore pressure induced bedding.	22
9. Sand and travertine dike.	23
10. Diagrammatic sketch of monoclinial structure.	25
11. Pinedale monocline.	28
12. Monoclinial fold and fracture zone.	29
13. Pipeline Canyon lineament.	30
14. Sowers' three-layer sandwich model.	35
15. Fractures in Dalton Sandstone.	38
16. Fractures in Cleary Coal Member.	39
17. Map of maximum principal stress directions in the United States.	46

## PLATES

- PLATE I. Measured Section
- PLATE II. Geology, Structure and Uranium Deposits of the Gallup  
1<sup>0</sup> x 2<sup>0</sup> Quadrangle, New Mexico and Arizona
- Plate III. Structure - Linear Summary
- Plate IV. Drainage Map
- Plate V. Lineament Map
- Plate VI. Geologic Summary and Surface Trend Map.
- Map A-1. Sample Locality Map

## GEOLOGY OF THE CHURCH ROCK SITE

### INTRODUCTION

The geologic investigation reported here was designed to provide support for the geohydrologic investigation of the Church Rock site, to provide detailed information on the evaporation pond sites, and for engineering considerations of structural stability of dikes and ponds. The large (4 quadrangle) area over which the structural, geologic, and fracture studies were conducted was necessary not only to provide adequate control for the definition of structural features, but also to provide the basis for possible future alternative site considerations.

The relatively short schedule and land access difficulties prevented examination of the entire area in detail. The geologic mapping and sampling approach used was to employ reconnaissance to locate accessible areas where critical features were exposed, and to study those areas in detail. Enough of the structural character of the area could be interrelated in this way such that an overall interpretation of the structural geology of the area could be constructed. When these interpretations were tested against mapping-in-progress, it was found that the structural character of the area is orderly and predictable within the area of study.

### STRATIGRAPHY AND DEPOSITIONAL HISTORY

The rocks exposed in the study area are within the Upper Cretaceous Mesaverde Group. They are, in descending order, divided into the following stratigraphic units:

Point Lookout Sandstone  
Crevasse Canyon Formation  
Gibson Coal Member  
Dalton Sandstone Member  
Dilco Coal Member  
Gallup Sandstone  
Mancos Shale

The thickness and lithology of each of the stratigraphic units are summarized in Table I.

These sedimentary rocks were deposited near the margin of a widespread Cretaceous epeirogenic sea under conditions characterized by more or less constantly changing shorelines as indicated by the complex intertonguing of nonmarine sediments to the northeast with marine sediments (Beaumont, 1971). In this area the marine Mancos Shale intertongues with coastal barrier sandstones and nonmarine deposits (Kirk and Zech, 1977; Molenaar, 1977a, 1977b) as a result of transgressions and regressions under subsiding conditions in the geosynclinal trough (Beaumont, 1971). Based on the lithology and sedimentary features, the sedimentary sequence in the area can be characterized by three major environmental facies (Fig. 1):

- Offshore Marine Deposits
- Coastal Barrier Sandstones
- Nonmarine Deposits

During the late Cretaceous, the initial westward incursion of the sea into the area was by far the most extensive. The D-Cross Tongue of the Mancos Shale represents a subregional transgression that separates the Gallup Sandstone into two parts. The lower D-Cross Tongue (Kmd1) in the study area (Plate I) includes a 6-foot thick fossiliferous sandstone which occurs approximately 60 feet below the lower Gallup Sandstone (Kg1). The frequency of the thin-bedded sandstones between this fossiliferous sandstone and the lower Gallup Sandstone increases upward indicating a gradual shifting of the shoreline seaward.

The lower Gallup Sandstone is probably the first regressive wedge in this area. The clay matrix in this unit decreases upward whereas the grain-size of the sand increases upward. At the top of the lower Gallup Sandstone, cross-bedding and ripple marks are present indicating that the lower Gallup Sandstone was deposited under littoral or nearshore and beach conditions.

TABLE I. Summary of Stratigraphic Units and Lithology in the Pipeline Canyon Area

Stratigraphic Unit	Thickness (feet)	Lithology
POINT LOOKOUT SANDSTONE	65 ±	Grayish-orange to very light gray, fine- to medium-grained, massive sandstone. Often crossbedded.
CREVASSE CANYON FORMATION Gibson Coal Member  Dalton Sandstone Member  Dilco Coal Member	180 ±  190 ±  150 ±	<p>Predominantly light gray shale with irregular, very light gray siltstone and fine-grained sandstone. Lenticular coals are common. One continuous coal seam (3-3.5 ft) is present. Lower half of unit is covered by colluvium or alluvium.</p> <p>Light gray, fine- to coarse-grained, massive, often fossiliferous sandstone. Irregular layer of conglomerate (0-8 ft) at top of lower unit.</p> <p>Upper part of unit consists of light gray to yellowish-brown, fine- to medium-grained sandstone and siltstone; light gray to dark gray shale and coal. Middle part of unit is massive, often crossbedded, fine-grained sandstone. Lower part of unit consists of dark gray, highly carbonaceous shale (near coals); light gray to grayish-brown shale where in contact with siltstone; light gray to grayish-brown shale where in contact with siltstone and thin-bedded, often ripple marked, sandstone.</p>

TABLE I (Cont'd). Summary of Stratigraphic Units and Lithology in the Pipeline Canyon Area

Stratigraphic Unit	Thickness (feet)	Lithology
GALLUP SANDSTONE	220 ±	<p>Upper Gallup--Upper part consists of light gray, fine- to coarse-grained, massive sandstone, often crossbedded; occasional thin beds of light gray, sandy shale. A continuous coal seam (0.5-2 ft) underlain by clay (3-5 ft) is traceable. Tree branch molds occur at the base of the unit. Lower part consists of light gray, fine- to medium-grained, massive sandstone, locally crossbedded near top of unit. A discontinuous band of iron staining (2-3 ft) occurs near the top. Average thickness ± 160 ft.</p> <p>The upper &amp; lower Gallup Sandstones are separated by the upper member of the D-Cross Tongue of the Mancos Shale, a thin-bedded shale, dark gray to gray, locally sandy.</p> <p>Lower Gallup--Medium light gray to very light gray, fine-grained, massive sandstone, locally crossbedded at top of unit. Clay matrix in sandstone decreases upward. Ripple marks are common near top of unit. Average thickness ± 60 ft.</p>
MANCOS SHALE	330 ±	<p>D-Cross Tongue--Dark gray to brownish gray shale; scattered thin-bedded, fine-grained sandstone and siltstone. Shale is fissile, with a calcareous zone, below the lower Gallup Sandstone and sandy between the upper and lower Gallup Sandstone. Locally, the lower part averages 150 ft, the upper part averages 80 ft.</p>

TABLE I (Cont'd). Summary of Stratigraphic Units and Lithology in the Pipeline Canyon Area

Stratigraphic Unit	Thickness (feet)	Lithology
		<p>Mulatto Tongue--Brownish-gray to gray sandy shale and thin-bedded, fine-grained sandstone. Locally, the Mulatto Tongue is split into a lower and upper tongue by the lower Dalton Sandstone.</p> <p>Fossils are common in both units in the shale and some sandstones. Ripple marks occur in some of the sandstones.</p>

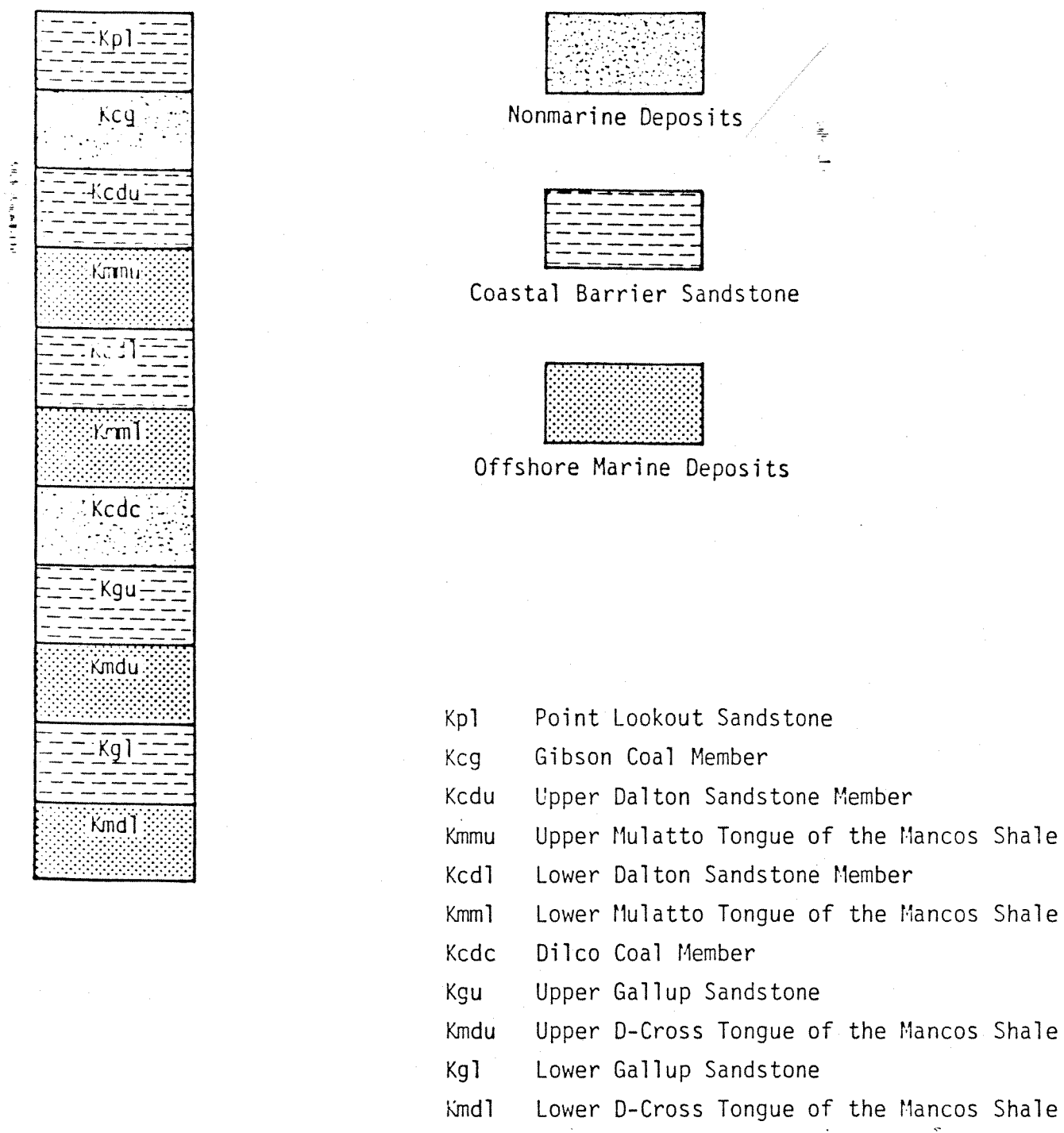


Figure 1. Generalized geologic section showing major environmental facies.

The regression seems to stop after the completion of the deposition of the lower Gallup Sandstone. A minor transgression followed by a minor regression then took place in the area. As a result, muds and thin layers of sand of the upper D-Cross Tongue were deposited. From the lithology of this unit, the advance of the sea reached its maximum near the late stage of deposition of the upper D-Cross tongue (Kndu). The sea then retreated rapidly from this area. An environment similar to that which prevailed during the deposition of the lower Gallup Sandstone also prevailed during the deposition of the upper Gallup Sandstone (Kgu).

Following the deposition of the upper Gallup Sandstone, the sea continued to retreat with minor fluctuations. From the nature of the crossbedding and lithology, the Dilco Coal Member (Kcdc) was deposited under fluvial and paludal conditions.

At the end of the deposition of the Dilco Coal Member, the sea advanced again and the lower Mulatto Tongue of the Mancos Shale (Kmm1) was deposited. The sea retreated before the deposition of the lower Dalton Sandstone Member (Kcd1).

The lower Dalton Sandstone Member is a typical regressive coastal barrier sandstone with local concentrations of marine fossils and an overlying conglomerate. The pebbles in the conglomerate were not derived locally, but were transported into the area during the transgression (Molenaar, 1973).

The upper Mulatto Tongue of the Mancos Shale (Kmmu) is also a transgressive marine deposit. This unit is much sandier and siltier than the lower Mancos Shale in this area. The increase of sand near the top of this unit is indicative that regression was taking place before the first deposition of the upper Dalton Sandstone (Kcdu) in the area.

During the retreat of the sea, the Gibson Coal Member (Kcg) was deposited under paludal conditions. The Point Lookout Sandstone (Kpl), however, is a depositional product of basal transgression as indicated by its lithology.

All of the units in this sequence thicken to the north. Structural control of sedimentation is evident in the pronounced local thickening of the sandstones. The Gibson Coal Member also thickens on the downward sides of the monoclinial folds in the area (Plate IIa; Map A-1, Location 40).

## REGIONAL TECTONICS

The site lies in the Colorado Plateau Tectonic Subprovince of the Rocky Mountains. The Colorado Plateau is bounded on the east by the Rio Grande depression and on the northeast by the Uncompaghre and Wind River Ranges. These northwesterly trending ranges are widely thought to be the remnants of Paleozoic or early Mesozoic subduction complexes. The Basin and Range terrain related to spreading along a north-northeasterly trending spreading axis defines the western boundary of a recognizable Colorado Plateau structural assemblage. The southern boundary is defined by a broad belt of right lateral movement on large features such as Walker's Lane and the Texas Lineament. Kinematics of the first order sub-plate motions are shown in Figure 2 as interpreted from Smith and Sbar (1974) and Coney (1976).

The Colorado Plateau has had the longest history as an intact crustal sub-block of any structural terrain in the southern Rocky Mountains. As such, it contains the most complex and temporally comprehensive structural assemblage in the region (Woodward, 1976). Although Paleozoic features which are probably influenced by structure are seen in the subsurface, the region was most strongly shaped in the period from late Cretaceous through the end of the Laramide orogeny (Miocene?).

The principal structural styles expressed in the region are basement strike-slip faulting followed by vertical block movements of basement rocks and associated folding of overlying sediment. Block movements are accomplished by high angle reverse upthrust faulting along relatively narrow zones. Relative block uplift and tilting is the most common local structural expression.

In some cases block margins show evidence that vertical motion has been superimposed on older strike-slip structural assemblages. In the case of some features (i.e., Gallup sag and Nutria monocline) there is evidence of oblique movements (Edmonds, 1961) which may be interpreted as transitional between these structural styles. Some workers have suggested that a continuous process

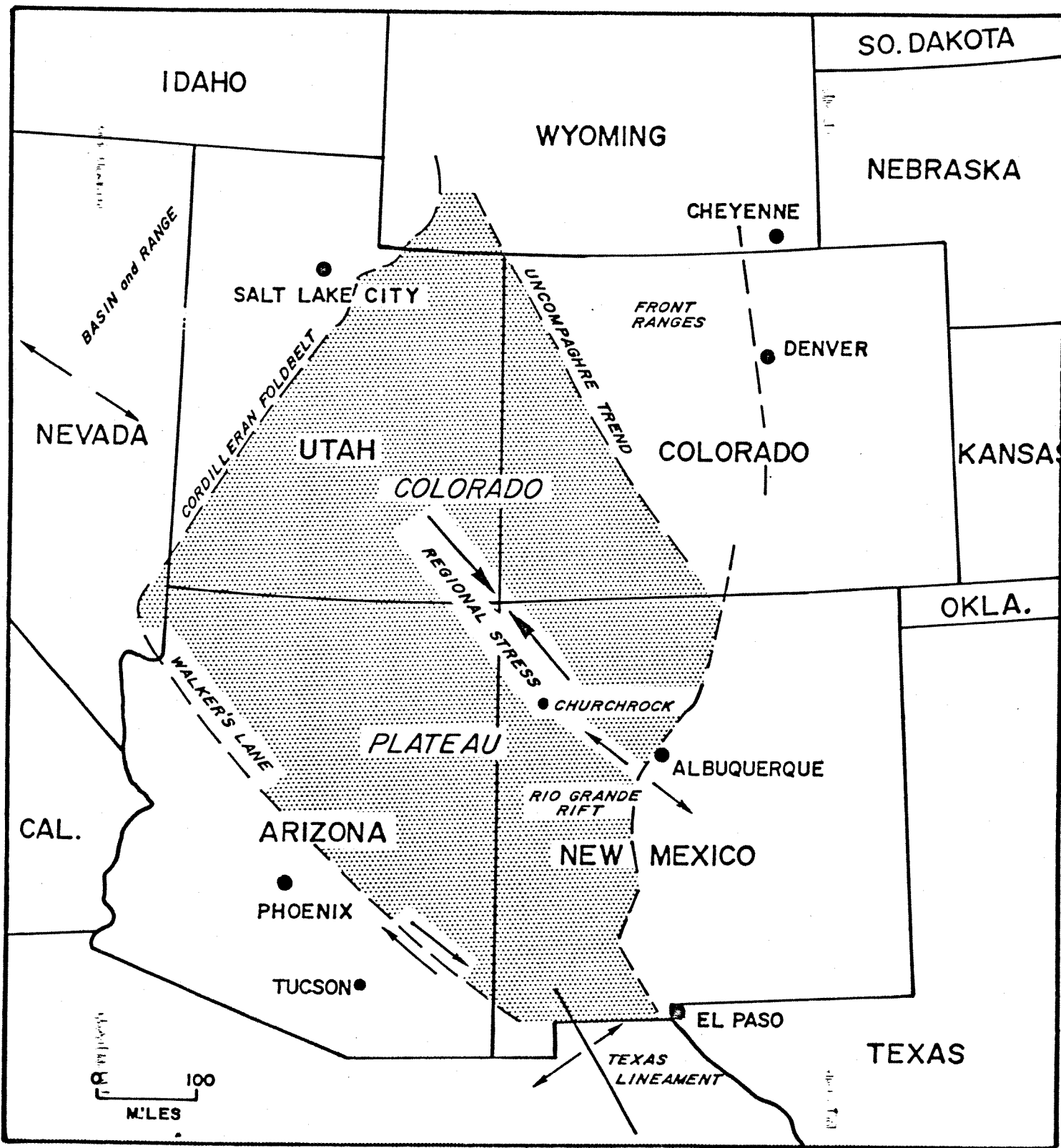


Figure 2. Boundaries and stress orientations of the Colorado Plateau plate tectonic subprovince - sketch map.

beginning with strike-slip faulting and vertical movements may result from transpression in response to local kinematic conditions along intersecting sets of regional strike-slip faults. Local crustal thickening and the kinematics of intersecting fault systems may have led to subsequent vertical block movement and tilting as a response to isostatic imbalance (Couples and Stearns, 1978; W. R. Muehlburger, 1979, personal communication; J. J. Prucha, 1980, personal communication).

One of the largest coherent basement blocks in the southern Colorado Plateau is the Zuni uplift (Plate IIb). The basement surface of the Zuni uplift is tilted gently to the north. Basement rocks are exposed at the southwestern corner of the uptilted block in the Zuni Mountains. The block apparently has a reasonably planar upper surface with few topographic irregularities interrupting the homoclinal, gently dipping nature of the pre late Cretaceous sedimentary rocks.

The Nutria monocline comprises the western boundary of the Zuni uplift. The Nutria monocline is an en echelon zone of sharp down-to-the-west flexing which separates the uplift from the complexly faulted and folded Gallup sag. Edmonds (1961) has suggested that the geometry of strain of minor structures along the monocline implies a right-lateral component to the otherwise ordinary upthrusting associated with monocline development in this region. The strain geometry of the Nutria monocline generally conforms to the style of other block uplift features in the Rocky Mountains.

The Gallup sag displays a structural geometry which implies development as the result of divergent (dispressive) movement along a strike-slip fault zone (D. A. Rogers, 1979, personal communication). Relationships between synthetic and antithetic faults imply right-lateral, strike-slip displacement along a broad zone which has subsequently been overprinted by the formation of the Zuni uplift, Chaco slope, and the San Juan Basin (Plate IIb). The local, relative uplift of the Zuni block has not been entirely uniform. Structures of much smaller displacement than the Nutria monocline-Gallup sag complex locally modify the edges and the interior of the uplift.

## LOCAL STRUCTURAL GEOLOGY

### INTRODUCTION

The United Nuclear Church Rock, New Mexico facility is located west of the Nutria monocline and south of the steepening of the regional dips into the San Juan Basin. In this sense the Church Rock site occupies the northwestern corner of the Zuni uplift.

### APPROACH

In order to provide a basis for the evaluation of fracture patterns in the site area, it was necessary to analyze the structural geology of the Church Rock site and its surrounding area in detail. No presently existing geologic map shows the structures of the area in sufficient detail to evaluate their origins and effects on rock permeability and character. The local control of permeability by fracturing along zones of faulting or bending of beds is a well known phenomenon.

A linear feature can be seen passing through or near the site area on ERTS imagery (Fig. 3), color aerial photography, and on subsurface geologic maps (Plates IIa, IIb). Two linears intersect within the site area at Church Rock, and a third (which trends northwest) passes a few thousand feet north of the pond area (Plates III, V). To establish the structural nature of these zones and their influence on fracture density, an area of four 7½ minute USGS quadrangles was studied. This was necessary to define the nature of the interrelationship among fracture patterns, linears, regional geologic structure, and the developmental history of the region.

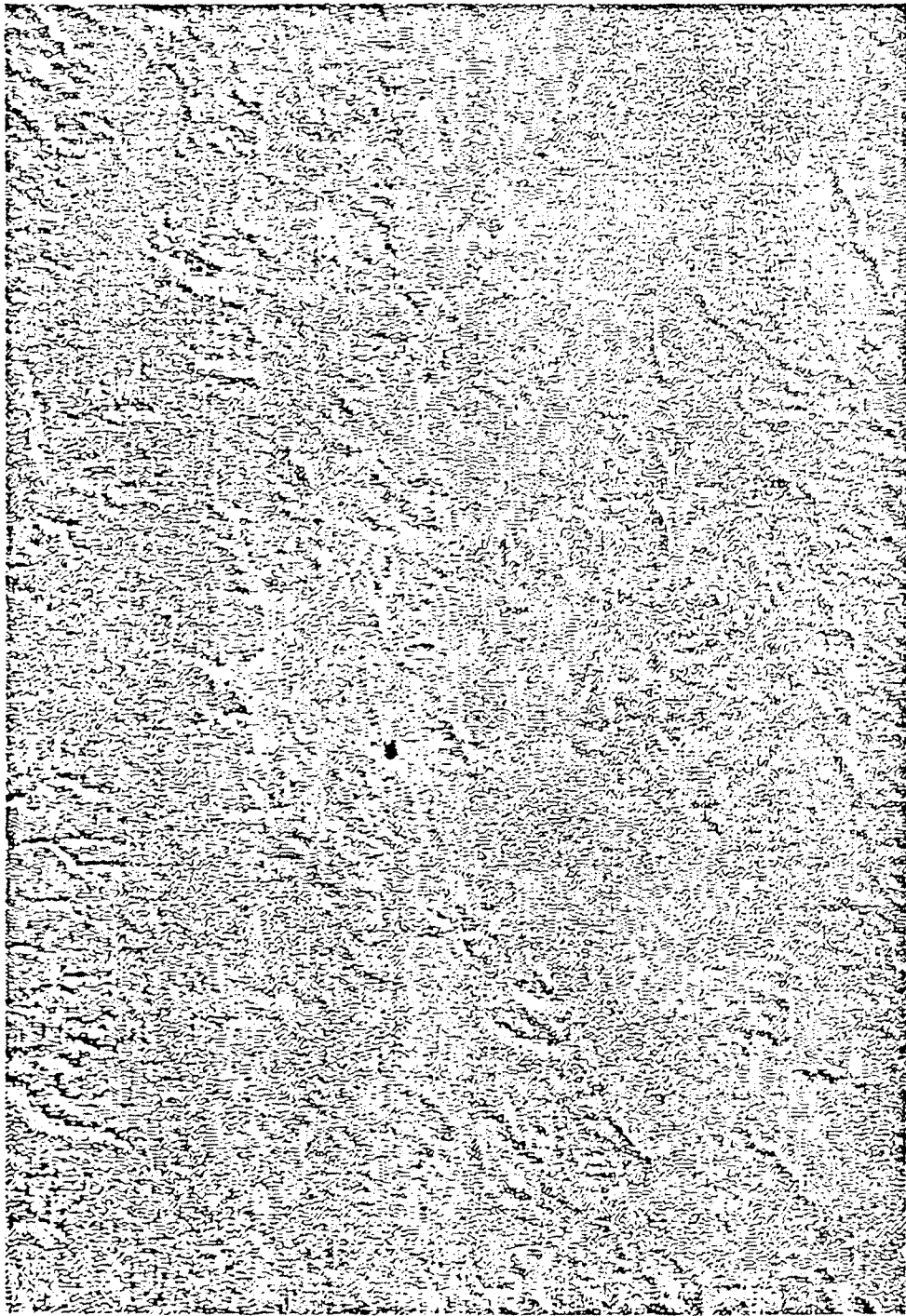
In order to quickly identify fracture zones associated with structural features, a combined program of photogeology, field reconnaissance, and detailed study of critical localities was undertaken. A photomosaic of the four 7½ minute quadrangles surrounding the site was prepared by Intrasearch, Inc. of Denver, Colorado. The mosaic was compiled from low altitude color aerial photography at a scale of 1/24000. This type of mosaic is called semi-controlled,

CHURCHROCK AREA, NEW MEXICO

The dot print begins at line 1760 and ends at line 2015  
The dot print begins at pixel 784 and ends at pixel 1293  
Channel 1, 5

Black = 6,000 White = 71,000

Scale =  100,000' 0 100,000'



● - SITE AREA

by: TECHNOLOGY APPLICATIONS CENTER  
University of New Mexico

Figure 3. ERTS imagery aerial photograph, Church Rock area, New Mexico.

in which flight path and position corrections are made but no effort is made to correct for purely photographic distortion. Individual aerial photographs taken by the USGS were used with the mosaic so that stereoscopic study techniques could be applied. The USGS photos were also used in the field and provided photo coverage at a different light angle than the mosaic, an aspect useful in photogeologic comparisons. The base map used in this report was prepared directly from the mosaic by photographic reproduction.

The Technical Applications Center (TAC) of the University of New Mexico compiled photogeologic overlays which characterize the drainage (Plate IV), lineament fabric (Plate V), and the attitude of bedding over the entire area (Plate VI). TAC was assisted by an SAI geologist who field checked geologic and geomorphic features. A second SAI geologist was engaged in field reconnaissance of all topographic, structural, and photogeologic features implied by the photogeology. A third geologist mapped in detail the Pipeline Canyon lineament and related geomorphic features from the vicinity of the old Church Rock mine to the northeastern terminus of the canyon.

Measurements of fracture attitudes and spacing in regions which were chosen to avoid linear elements or changes in the structural attitude were pursued simultaneously with the structural study. This was done to provide a sample of the regional fracture pattern.

Sample traverses perpendicular to the traces of prominent structural zones or linear features were carried out where cover conditions and land access arrangements permitted. These were designed to identify and characterize fracture distribution in fracture zones which might be associated with lineaments and/or structural zones which pass through the site area.

Conditions of erosion, plant and soil cover, and land access difficulties make the complete characterization of the fracture patterns in any given area impossible. Techniques for extrapolating known fracture distributions over unsampled regions have recently been developed (Harris, 1960; Gibbons, 1962, 1980; Price, 1966; Sowers, 1973; and others). Some assumptions about lateral variation of rock properties, thickness and environmental conditions were

necessary, as in any geostatistical approach. Conservative handling of data and assumptions make this an approach which can be used to generate theoretical limits for fracture distribution. This approach can be used with confidence in a gently, simply deformed area like the site area. Results of the fracture study and discussions of sampling and data handling techniques are presented in Appendix A.

## STRUCTURAL GEOLOGY OF THE SITE REGION

Several structural zones impact the study area (Plates IIa, IIb). These structural zones are characterized by monoclinal folds which effect changes of the strike of bedding across the trends of the folds (Plates III, IV, VI) and second order features which are oblique to the main trends of the folds. These relationships imply some rotational strain as the result of oblique movement. These monoclines are not always simple structures. They occasionally display slightly sinuous or en echelon character (Pinedale monocline) and more than one hinge (Fig. 4). Two of the principal structural zones in the area can be traced to their intersection with Nutria monocline. The intersections are coincidental with changes of strike in the Nutria monocline (Plate IIa). The Nutria monocline is a first order regional feature which forms the western boundary of the Zuni uplift. It has been interpreted (Edmonds, 1961) to be a monocline associated with a steeply-dipping reverse fault of the upthrust type. Minor structures also display evidence of right-lateral movement coincident with upthrusting (Edmonds, 1961). The upthrust structural style is the structural style of large areas of the Front Ranges, the Colorado Plateau, and the Rio Grande depression (Prucha, *et al.*, 1965; Woodward and Callender, 1977; Couples and Stearns, 1978).

The geometry and kinematics of all of the structural features present in the area are commensurate with the interpretation that the site area is at the northwestern corner of the Zuni uplift which is a structural terrain dominated by upthrusting and block tilting.



Along the lineaments within the site area (Plates III, V) no discrete dislocations directly related to basement faulting have reached the present level of structural exposure. The considerable thickness of young sediments, the presence of weak and ductile evaporite rocks at depth, and the very small total structural relief across these features strongly imply that the monoclinical folds were the results of passive drape folding.

#### STRUCTURAL GEOLOGY OF THE SITE

The site lies in the vicinity of three structural zones. Two of these features are the central, east-northeastward trending leg of Pipeline Canyon (Plate III) and the north-northeastward trending Fort Wingate lineament. The largest structure in the site area, the Pinedale monocline, trends to the northwest and passes to the northeast of the site. The Pinedale monocline is a complex monocline with two hinge zones (Fig. 4, Plate III), as is common in monoclines related to upthrusting (Prucha, *et al.*, 1965). Total structural relief across the structure on the upper surface of the Dalton Sandstone is between 60 and 125 feet. Most of this structural relief is compensated by thickening in the Gibson Member. A slight flexure is apparent at the bottom of the Point Lookout Formation in the head of Hardground Flats Canyon and in the next canyon east. This implies that passive monoclinical folding may have continued into Point Lookout time. There is some controversy on this point, however. Robert Zeck (1980, personal communication) of the USGS interprets all linear elements parallel with the Point Lookout and Cleary Coal (?) depositional strike to be purely paleogeomorphic in origin. The traceability of the Pinedale monocline into a linear element of post Point Lookout age implies that some interaction existed between structural and ancient shoreline geomorphic processes. The presence of sand dikes and local flexure along ancient shoreline features strongly argues for the association. The locus of upthrusting and deposition in the site area had shifted northward on the Chaco slope at the end of Point Lookout or Cleary Coal time.

The two structural features (Plate III) which pass through the site area are both complex structural zones made up of a persistent but small (3-4 degree) change in regional dip. Regional strike changes across both zones imply some rotational movement. Subsurface data (Plate IIa), field relationships and analogy with comparable structural styles support the interpretation that a rotational sense of movement on the basement faults was responsible for passive monoclinial flexure at the present elevation of structural exposure. The two structural zones cannot be precisely located through the site area due to lack of exposure. Elements of both structures can be traced to within several hundred feet of the site area on the south. Geomorphic control and a local breccia exposure locate the northern end of the Pipeline Canyon lineament within several hundred feet of the northern boundary of the site (Plate III). The Fort Wingate lineament is not expressed beyond its intersection with the Pipeline Canyon lineament near the north end of the site. This may be its true terminus under the thickening sedimentary sequence or it may indicate the formation of a composite trend.

#### STRUCTURAL-DEPOSITIONAL HISTORY

The axis of deposition in the region trended approximately east-west and lay along a series of shorelines which are marked by beach deposits and dune sequences across the area. In general, all units thicken rapidly to the north. Locally the thicknesses of the sandstones is controlled by monoclinial warping (see preceding section). All structural features become less distinct and exhibit less structural relief as they are traced northward. Structures implying high pore-water pressures are often associated with monoclines (Figs. 5-9). The Pinedale monocline can be seen to decrease in structural relief in direct relationship to the thickening of channel sands and coals of the Gibson Coal Member at Location 40 (Map A-1). These features and other field observations dictate the conclusion that the subsurface upthrust faulting and associated monoclinial folding were syndepositional.

#### MONOCLINAL FOLDING

The monoclinial folds were formed by the passive bending or drape of the young sediments over the structural relief generated by basement faulting.



Figure 5. View of a sand dike in the Pipeline Canyon fault, looking northeast (Site 33, Map A-1).



Figure 6. View of a sand boil diapir (or drainage nodule) in Pipeline Canyon; width is approximately 4 ft; note the contortion (Site 33, Map A-1).

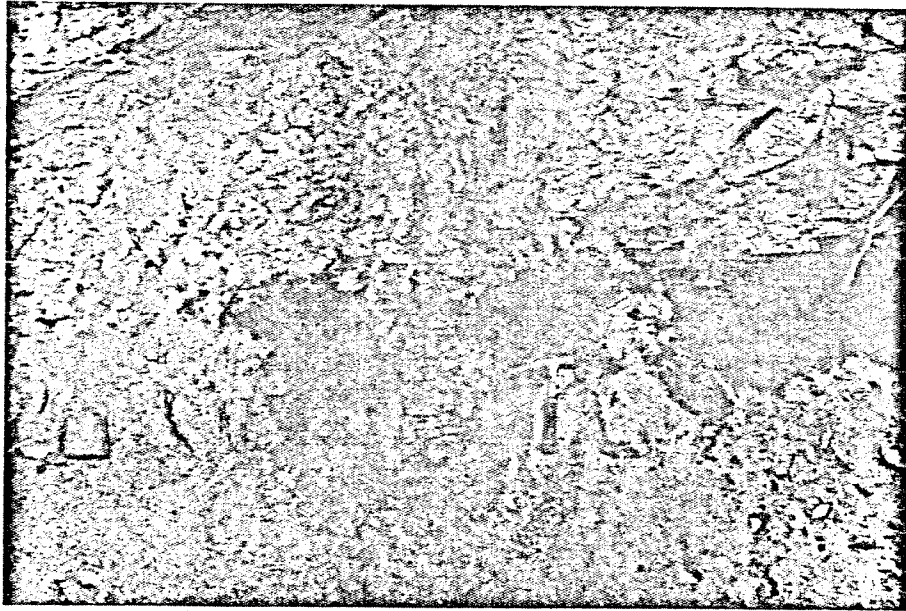


Figure 7. View of a sand dike through one of the coal layers in the Menefee Formation (?), looking east (Site 34, Map A-1).

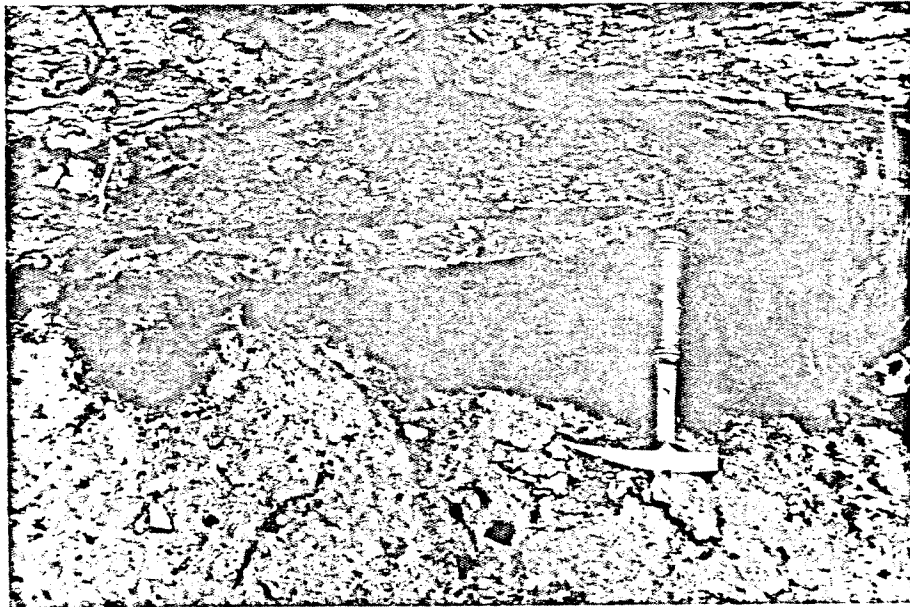


Figure 8. View of high pore pressure induced bedding in the Menefee Formation (?), looking east (Site 34, Map A-1).



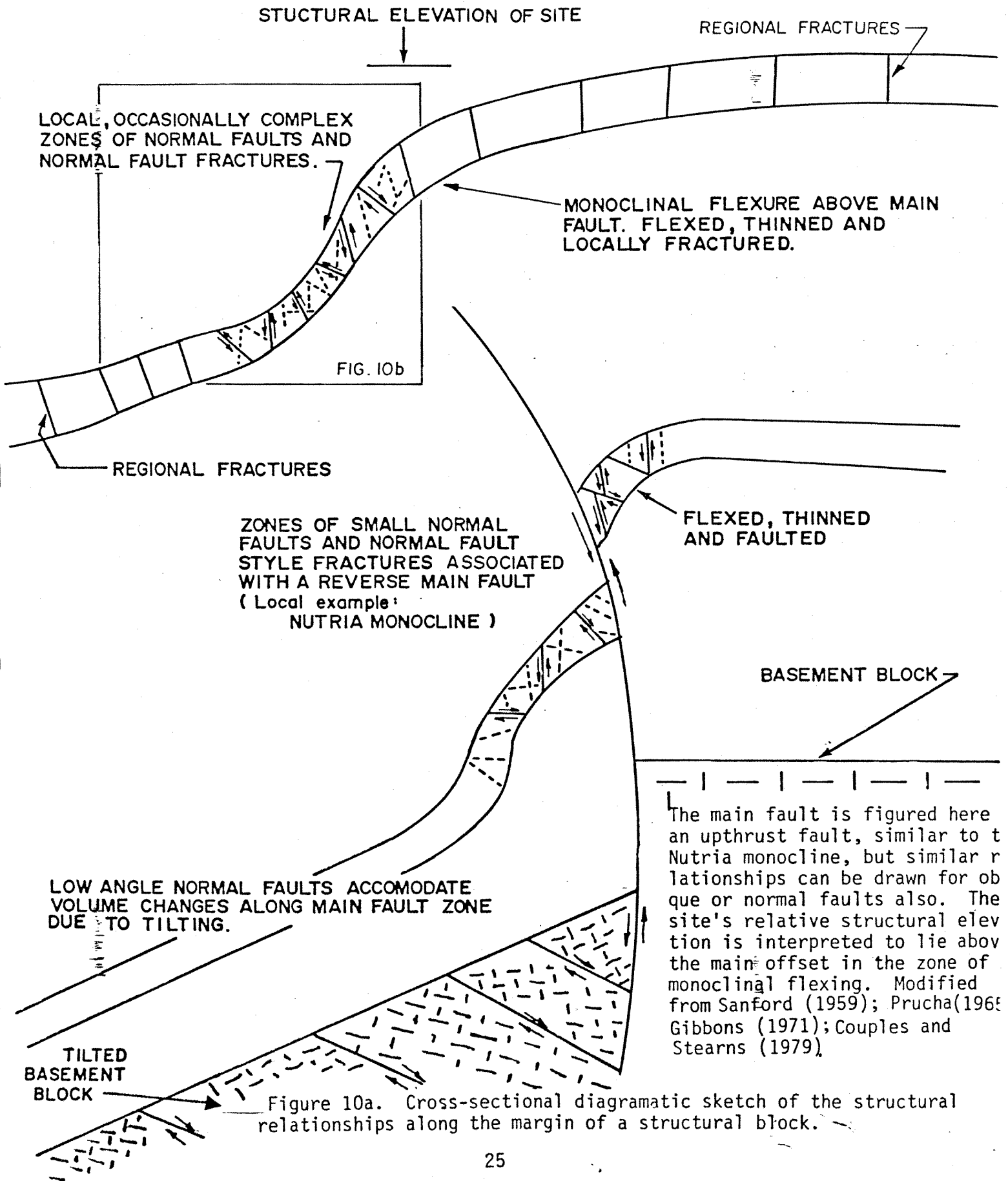
Figure 9. View of a sand and travertine dike in the Pt. Lookout Sandstone, looking north (Site 35, Map A-1).

local extension was generated in the hinge areas of the monoclines by the spatial requirements of a propagating bend (Fig. 10a). Local, very small faults have formed in brittle sandstone beds as the result of the local extension across the monoclinial hinge (Fig. 10b) and are not continuous through the interbedded shales. These faults are normal faults whose strike (north) is oblique to the strike of the monocline (northeast).

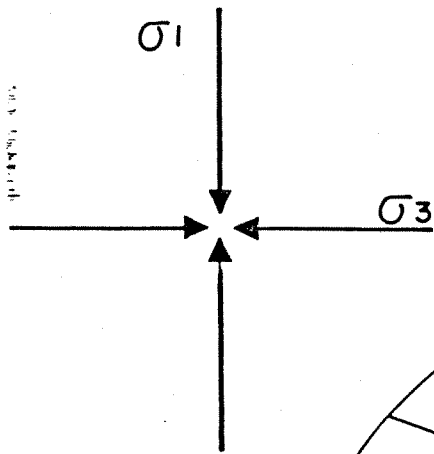
#### AGE OF MONOCLINAL FOLDING

All structural features recognized are associated with the monoclinial folding or the regional fracture pattern. The intimate association of all structures with sedimentation patterns and with the evidence for high pore-water pressures strongly implies a late Cretaceous or early Tertiary age for this terrain. The lack of structural features which do not fit into the geometry and kinematics of the regional structural style further reinforces the above interpretation of the relative age of the structural terrain.

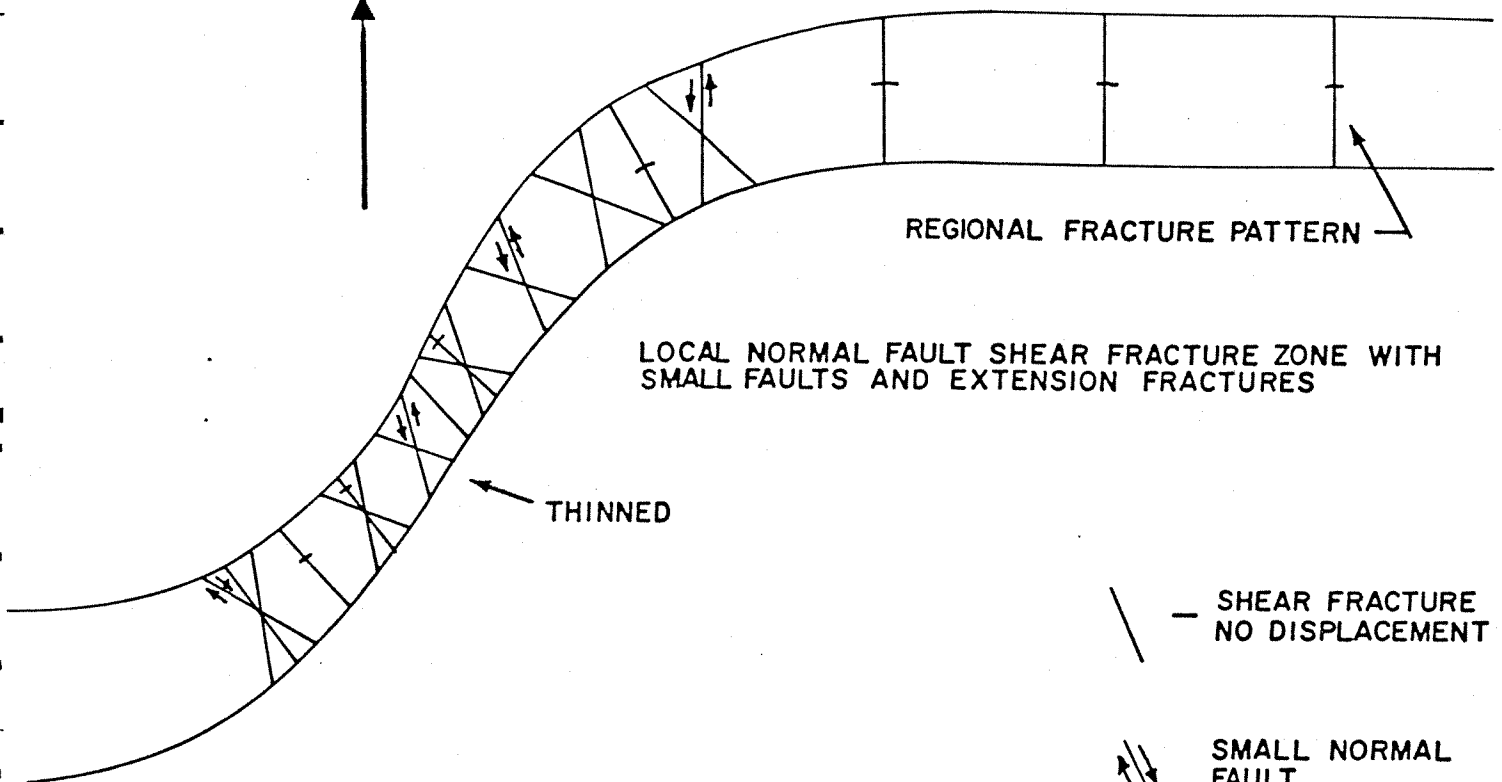
Each of the major lineaments on the map reflects a monoclinial fold and/or second order features associated with the monoclinial folding (Plates III, VI). The Fort Wingate lineament occurs as a photolinear and as a shear fracture zone in the area of study (Plate III) but can be followed southward into a slight flexure which aligns with the trace of the Fort Wingate fault (Plate IIa). This relationship implies that it is structurally similar to and approximately the same age as the other features at the site.



SUPERINCUMBENT  
LOAD



$\sigma_1$  (Superincumbent load)  $>$   $\sigma_3$  (Static Horizontal stress) - EXTENSION DUE TO STRETCHING BEDS OVER MONOCLINE



LOCAL NORMAL FAULT SHEAR FRACTURE ZONE WITH SMALL FAULTS AND EXTENSION FRACTURES

REGIONAL FRACTURE PATTERN

THINNED

— SHEAR FRACTURE  
NO DISPLACEMENT

— SMALL NORMAL  
FAULT  
ARROWS SHOWS  
SENSE OF STRAIN

— EXTENSION FRACTURE

THE TOTAL STRAIN ( thinning ) IS A FUNCTION OF STRUCTURAL RELIEF OF THE FEATURE RELATIVE TO ITS 1/2 WAVELENGTH

Figure 10b. Detailed schematic cross-section of structures associated with monoclinial flexure.

## FRACTURE PATTERNS

### INTRODUCTION

Local fracture patterns associated with structural zones have been discussed in the foregoing section. A summary of their geometry and distribution will be presented at the end of this section in the summary discussion of the composite fracture pattern of the region.

### EXTENT OF LOCAL FRACTURE PATTERNS AT THE SITE

The geometry of local fracture patterns at the site is closely related to the geometry of monoclinial folding. The intensity of fracturing in the hinge or hinges of the fold is directly related to the sharpness and magnitude of bending. Fracture zones tend to be a few hundreds of feet wide and trend parallel to the fold axes (Figs. 11, 12).

The local fracture patterns which cross the site area are associated with the Fort Wingate lineament and the Pipeline Canyon lineament. The Pipeline Canyon lineament ends its geomorphic expression at the northern end of Pipeline Canyon. Subsurface (Dakota) expression of structural relief associated with the lineament terminates just northeast of that point. This is consistent with the rotational geometry of the feature (Fig. 13) and with the interpretation of the lineament as the surface expression of a minor fault which segments the edge of the Zuni uplift. The Fort Wingate lineament is similar in all aspects to the Pipeline Canyon lineament. The feature in the site area appears to be the northern expression of the Fort Wingate fault and monocline (Plate IIa).

### REGIONAL FRACTURE PATTERN

One of the principal characteristics of rapidly accumulated shale and sandstone sequences throughout the Rocky Mountains region is a regional orthogonal fracture pattern (Harris, *et al.*, 1960; Stearns, 1968; Prucha, *et al.*, 1965; and others). Such patterns generally consist of two sets of fractures which are essentially perpendicular to bedding and to each other. Plumose surface structures, fracture geometry and relationship to other kinematic elements identify these features as extension fractures.

1000000000

1000000000



Figure 11. View of the crest of the Pinedale monocline, looking northeast (Site 31, Map A-1).

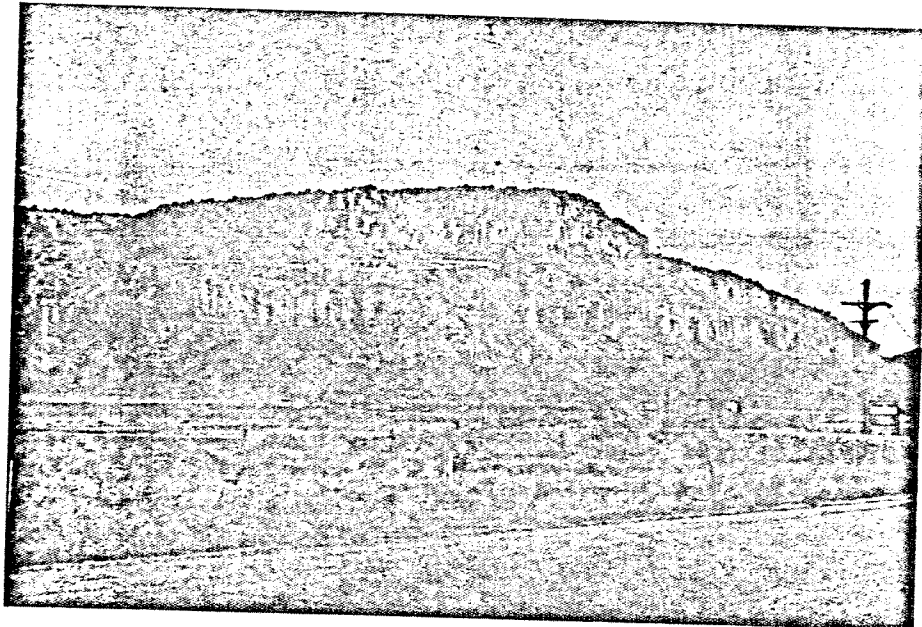


Figure 12. An oblique view of the fracture zone along the hinge of a monoclinical fold, a second order feature associated with the Pipeline Canyon fault; view to the northwest from Hwy. 566 (Site 36, Map A-1).

00000000

00000000



Figure 13. View to the southwest across the Pipeline Canyon lineament illustrating the change in regional dip (Site 37, Map A-1).

## FRACTURE ZONES ASSOCIATED WITH MONOCLINES

Steeply-dipping, normal fault style shear fractures are diagnostic features of the hinge zones of the monoclines. The development of a shear fracture component of the fracture pattern in these zones indicates transitional strain behavior during folding. This implies that the monoclines developed after dewatering had progressed to the point that the brittle behavior resulting from high pore pressures had diminished. There is a strong correlation between monoclinial features and the observed sand dikes. The strikes of the sand dikes parallel the traces of the associated monoclines. These relationships imply that dewatering was not complete when the monoclines formed (Figs. 5, 7, 9).

The degree to which the fracture zones resulting from monoclinial bending can be characterized by this study is limited. Not all strain associated with monoclinial folding is expressed solely as shear fractures. Some stress is expressed by other strain mechanisms. Some elasticoviscous flow certainly accompanied the formation of shear fractures, and extension on both old (regional) and new extension fractures may have contributed to the total strain. The percentage of total strain represented by shear fractures cannot be estimated because of these uncertainties. The zones along the monoclinial hinges have suffered preferential erosion because of the more dense fracturing, thereby preventing complete fracture sampling traverses across the features.

Fracture zones associated with monoclines are a few hundreds of feet wide and are closely associated with the hinge or hinges of the fold (Fig. 11). Most of the fractures which are associated with monoclines strike parallel to the fold axis or are at a small angle to it. Interpretation of these examples and of other, more fragmental sample traverses indicates that the fracture zones associated with these monoclines display an overall normal density distribution with regard to total fractures and for steeply dipping shear fractures along a traverse perpendicular to the trace of the monocline (see Appendix A, Figs. A-18, A-19 and A-21). The regional fracture pattern averages one fracture per 10 feet over most of this area. The maximum number of fractures observed on counting traverses across monoclinial trends was 10 per 10 feet. (Note: Sixteen fractures per 10 feet was estimated from a partial traverse; see Appendix A, Fig. A-21).

## DISTRIBUTION OF REGIONAL FRACTURE PATTERNS

Regional orthogonal fracture patterns tend to be very consistent in geometry over large areas of slightly deformed, homoclinally dipping rocks. Often, local domains related to basinal margin geometry or the trends of isopach lines display orientations and spacings which are remarkably statistically consistent (Price, 1959; Sowers, 1973; Woodward and Callender, 1977; Appendix A). Fracture spacing is profoundly affected by bedding thickness and lithology but in the study area fracture distribution was remarkably consistent within individual sandstone members.

Regional orthogonal fracture patterns occur over large areas in which they are the only structural features. Regional orthogonal fracture patterns are commonly associated with evidence for rapid dewatering (Secor, 1968; and Gibbons, 1980). Theoretical developments by Secor (1968) and by Robinson (1959) have led to the conclusion (Gibbons, 1980) that regional orthogonal fracture patterns in rapidly accumulated, nearshore sedimentary suites are the result of hydrofracturing of rocks under the load imposed by burial. Shale and coal interbeds acted as aquacludes retarding the dewatering rates of the sandstones. The resulting rise in interstitial water pressure directly countervenes the lateral confining pressures, allowing the total superincumbent load to be applied as effective stress leading to extension fracture (Secor, 1968). High pore-water pressures further increase brittle behavior since overpressured water enhances extension fracture via the effects of Griffith's Law (Secor, 1968). Body stresses due to basinal configuration, active or remnant tectonic stresses are sufficient to ensure a triaxial stress state.

The mechanics of the development of the details of regional orthogonal fracture geometry are presented in detail by Price (1959). The site area is situated in a region in which all the environmental criteria and field evidence support the existence of a regularly distributed, geometrically consistent network of regional orthogonal fractures. Inasmuch as these fractures presumably originated to allow the expression of water under depositional loading, they must be presumed to have originally been, to some extent, interconnected. The domain over which this fracture pattern exists is larger than the area of study.

## SOWERS CALCULATION

Fracturing is one type of response where the stress environment exceeds the strength of the rock. To a certain degree, the physical properties of the rock unit affect this response. The majority of geologic studies of fractures have been limited to inventories and typologies of fracture patterns. Of the many aspects of fracturing and faulting, the area of fracture spacing is among the least developed.

As early as 1947 Russian geologists observed that fracture spacing in beds undergoing extension is inversely related to the thickness of the rock unit (Belousov, 1962). Harris, *et al.*, (1960) studied two major structural features in northern Wyoming (an anticline and a dome) and also observed that fracture spacing in sedimentary rocks is inversely related to bedding thickness.

Price (1966) and Hobbs (1967) attempted to model fracture spacing using classical theoretical methods. Again, they both found that fracture spacing is inversely proportional to bedding thickness. Price postulated that the stored elastic strain energy which created new surfaces as it was released played an important role in a fracture spacing. Secor (1968) suggested that many extension features are caused by the mechanism of hydraulic intrusion. For all of these theories to work, large viscous flow is required.

The Sowers (1973) approach does not require large viscous flow, focusing instead on the stability of layered media undergoing extension using strain energy methods. His work represents the first concentrated effort to develop a quantitative theory that can be used in modeling fracture spacing. More importantly, he demonstrates that, using strain energy methods, the ability to predict the occurrence of some fracture patterns is possible. He posits that fracture spacing may be controlled by elastic stress concentrations. In compressed, layered rocks the initial uniform stress field may become unstable and periodic stress concentrations may develop. The instability, which is caused by differences in the mechanical properties of the layered sequences, is initiated by a critical stress. If this stress exceeds the strength of the rock, fracture occurs. These stresses are often periodic and their frequency serves to localize fractures.

By using strain energy methods, the elastic moduli for anisotropic materials need not be known; also, the elastic stress fields or displacements which have occurred prior to fracture are not needed. Sowers uses the principle of virtual work

$$\Delta V - \Delta W = 0 \quad (1)$$

to find the critical tension,  $T$ , for elastic instability. We can see from Eq. 1 that  $\Delta V$ , the incremental strain energy stored in the system, must be equal to  $\Delta W$ , the work done by the external forces for the incremental deformation. Experimentally,  $\Delta W$  is determined by finding the change in the length of a beam,  $\Delta L$  (caused by the sinusoidal surface loading), multiplied by the tension,  $T$ :

$$W = T\Delta L \quad (2)$$

He ultimately derives the equation (modified here)

$$W = (2BL + \frac{TL}{E}) \frac{T}{t} \quad (3)$$

where,

$B$  = amplitude of sinusoidal perturbation

$L$  = deformed length of beam

$T$  = applied tension

$E$  = Young's modulus of elasticity

$t$  = thickness of bed.

Sowers conducted experiments on photoelastic gel models which verified the fracture spacing intervals which the above theory predicted. A three-layer sandwich model was used in which a thinner, brittle layer was placed between two thicker layers of a more ductile material (Fig. 14). Multiple layers of alternating clay and putty were also tested. His observations are summarized as follows:

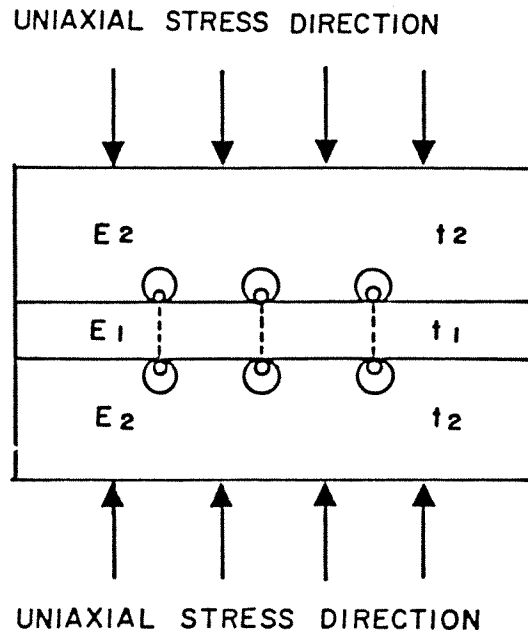


Figure 14. Three-layer sandwich model. Early indication of instability; small concentric circles indicate high stress concentrations that appear before the fractures occur. Fractures will appear along dashed lines,  $E_1 > E_2$ ,  $t_1 \gg t_2$  (Sowers, 1973).

1. When contacts are welded, stress concentrations are larger and more closely spaced and the number of fractures increases.
2. Instability occurs only when  $t$ ,  $E$ , and  $L$  are such that tensile stresses exceeding the critical value can occur prior to fracture.
3. Because of multiple modes of fracture, spacing at the end of an experiment is variable; first formed fractures are rarely perfectly spaced and vary from predicted spacing in experiments by a considerable amount.
4. Tests made with free interfaces or low frictional contact have few or no fractures which dramatically shows the influence of interfacial shear on the formation of the instability.
5. When tension is plotted against only normal surface forces, fractures increase linearly with tension; but, when tension is plotted against shear forces only, fractures are inversely related to tension.

6. Overall, fractures are more frequent in thin layers than in thick ones, other things being equal.
7. As stress dies out exponentially away from the surface of the embedding medium, the effects of thickness are most important in thin layers; for example, the critical tension for a 5-mm layer sandwiched between two 5-mm layers is about half that for a 5-mm layer bounded by two 50-mm layers.

Hobbs (1967) showed, theoretically, that fracture spacing is inversely proportional to the square root of Young's modulus ( $E$ ) of the bed; however, Sowers' experimental results indicated that spacing does not appear to be sensitive to changes in  $E$  for materials of the same hardness. Harris, *et al.* (1963) noted that calcareous quartz sandstones yielded higher fracture densities than friable quartz sandstones. While it is acknowledged that the mechanical and physical rock properties contribute to fracture spacing, the full extent of these effects have not yet been studied extensively. Stearns (1968) cites evidence from Handin, *et al.* (1963), that for a structure that was deformed under at least 10,000 feet of overburden, the fracture spacing index for silica cemented sandstones is half again as great as that for calcite cemented sandstone.

The study area presented an excellent opportunity to field test Sowers' three-layer model and the theory that fracture spacing is proportional to thickness. Sandstone beds of apparently similar lithology but different stratigraphic position and thickness are everywhere embedded between sandy shales. The results correlated poorly with Sowers' predictions. The pattern of variance was not simple, but it appeared that in general fracture frequency decreased upward in stratigraphic order. This may imply that smaller loads or that different paleogeohydrolic conditions persisted in the upper beds relative to the lower beds. Physical properties must have varied considerably in the sandstones as packing and degree of cementation changed during the compaction process.

A method for extrapolating fracture spacing based on Sowers' theoretical model is not possible at this time. Field methods for determining  $\Delta V$ , the strain energy, are not adequately developed and further theoretical development of

Sowers' approach is not within the scope or schedule of this project. As a result, a more qualitative approach was adopted. It must be noted that all previous field work has been limited to relatively thin rock units, and that, with the exception of Harris's study, only one kind of sandstone was sampled. Additionally, previous studies were confined either to a very small area, or, as in the case of the Harris study, the rock units were continuous over a wide area.

Figures 15 and 16 are photographs of lensoid bodies of sandstone which vary in thickness over relatively short distances. The variation in fracture spacing relative to bed thickness is evident and provides a basis for empirical reasoning useful in predicting fracture spacings in the subsurface at the site. The generally consistent relationship which can be interpreted from these and other similar localities, is that fracture frequency is inversely proportional to bed thickness or group of beds having similar stratigraphic position and lithology.

#### RELATIONSHIP OF FRACTURE SPACING TO ROCK TYPE AND BED THICKNESS

Regional orthogonal fractures are spaced at an average of 1 per 10 feet apart in sandstone beds 20 to 30 feet thick and strike north-northeast and west-northwest. Relative distribution of the two sets is not necessarily consistent at any one site, but average spacings over long traverses in one unit, parallel to depositional strike, are remarkably consistent (Appendix A).

The regional fracture pattern varies in its spacing. In general, fracturing should become less frequent to the north in proportion to the thickening of lithologic units. Sowers (1973) demonstrated that where known, purely extensional strains can be interpolated to yield fracture spacings in beds of different thickness and character if the thickness and physical properties of the rock are known.

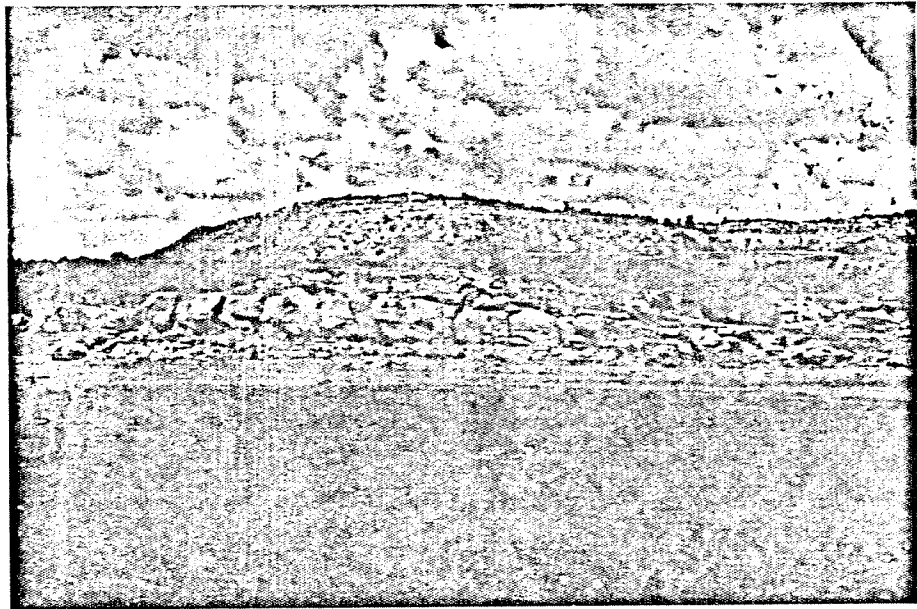


Figure 15. View to the west of an outcrop of the Dalton Sandstone (in the foreground) approximately 0.5 miles northeast of the site; note the fracture spacing vs. thickness of the unit (Site 38, Map A-1).

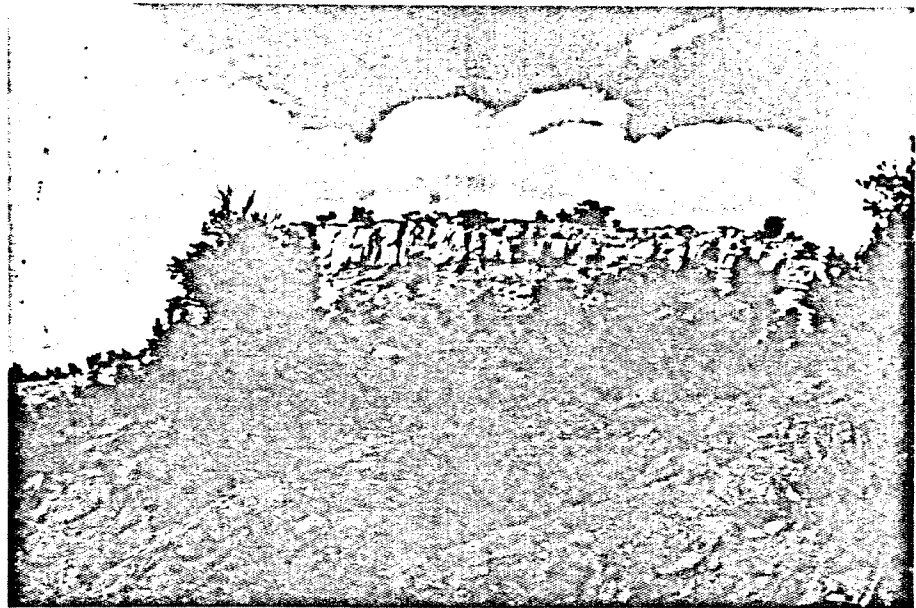


Figure 16. View to the east of a sandstone unit in the Cleary Coal Member north of the site; note the fracture spacing vs. thickness of the unit (Site 39, Map A-1).

## RELATIONSHIP OF PHOTOLINEARS TO FRACTURE PATTERNS

Study of photolinears in the region was compared to measured orientations of fractures. In areas between principal lineaments associated with monoclines the agreement among orientations of measured fracture patterns and short photolineaments was excellent (Appendix B and Fig. A-3). Fracture plots from localities in the vicinity of major lineaments, including known structural zones, display organized groups of fractures and lineaments which are not related to the regional orthogonal fracture pattern (Figs. A-7 and A-9). These non-regional fracture sets are related to the local fracture zones associated with the structural zones. The regional lineament pattern and the measured orientations of regional orthogonal fractures agree throughout a wide area. This agreement strengthens the interpretation that the measured data represent a fracture pattern of wide and consistent distribution overprinted by local fracture patterns associated with specific structural zones.

### SUMMARY

The regional fracture pattern is made up of two orthogonal sets of extension fractures which are due to hydrofracture during compaction. The sets strike north-northeast and west-northwest and are very regular in geometry and spacing. Because of variance in load, or because of related variance in the paleogeohydrologic field, the lowermost sandstone in the site area (lower Gallup Sandstone) appeared to be more densely fractured than the sandstones above it. In any case, the average spacing of regional orthogonal fractures (1 fracture per 10 feet) is not affected by the slight difference in fracture spacings relative to stratigraphic position. The regional fracture pattern is expected to change as the sandstone and shale units thicken to the north. The thickness of individual units is at least doubled over short distances. This implies that the average regional orthogonal fracture spacing increases to the north.

Local fracture patterns vary similarly with the regional fracture pattern with respect to thickness. The situation is complex in terms of predicting fracture type and densities in local fracture patterns. The strain field in

these passively deformed sediments varies with position on the structure, depth to the basement, and tectonic rate of strain. Other factors which affect regional fracture spacing affect local fracture patterns as well. Difficulty obtaining complete samples across local fracture zones further limits the degree to which local fracture patterns can be characterized.

The available information implies that the local fracture zones associated with the structural zones at the site are a few tens of feet to several tens of feet in width. The fracture zones may be made up of parallel or en echelon discrete sub zones (Fig. 4), or it may be a single, coherent zone (Fig. 12). Minimum spacing may be as small as 20 to 30 fractures per 10 feet. Two fracture types appear to be characteristic of local fracture zones. Vertical extension fracture and high angle normal-fault style shear fractures appear in varying proportions.

The highest fracture density in the region occurs along the structural zones where the local and regional fracture patterns are overprinted. All types of fracturing probably become more widely spaced to the north of the site as lithologic layers thicken. The local fracture zones related to the two structural zones which pass through the site appear to terminate along strike to the north-east. This is probably due to a termination of the basement structures with which they are associated as well as to the northward thickening of the sedimentary sequence.

Individual fractures in the sandstones are not continued through the shales below the sandstones. Fractures in the shales are generally tightly closed due to the weakness and ductility of the shales under the stresses imposed by gravity.

## HYDROGEOLOGIC IMPACT

Most geohydrologists who have attempted to model fracture flow do not include shear fractures in assessing the total impact of fracturing on transmissivity (O'Neill, K., 1977; James V. Dugid, 1979, personal communication). The tendency for shear fractures to have both faces in contact and the tendency to exhibit filling of the fracture with gouge are cited as the rationale behind such reasoning. In reality, most rocks may exhibit three classes of change in transmissivity as the result of strain.

Strain may affect interstitial permeability, may introduce large fracture openings by extension fracture, and may induce new permeability by the creation of very narrow fracture passages by shear fracture. Shear fractures are primarily capable of passing only very thin films of fluid or air, but they may, when sufficiently dense, alter the transmissivity of rock. The widespread association of clastic dikes with the axial regions of flexures and with local faulting in hinge areas strongly implies that the fracture zones in those areas influenced permeability during the dewatering of the sediments of the region.

Where local fracture zones are superimposed on the regional fracture pattern, the most dense fracturing was observed (Figs. 4 and 12, Plate III). These zones are also highly directional in development, showing a pronounced preferential development of fractures which strike parallel or nearly parallel with the trace of the axis of monoclinal folding. Quantitative characterization of changes in transmissivity along such zones is not solely related to the order of magnitude change in fracture frequency across such zones (1 fracture per 10 feet versus 10 fractures per 10 feet). Fracture type, fracture opening, fracture fill, and the nature of hydrologic communication between fractures strongly influence the effect of such a zone. Direct field measurement of hydrologic conductivities in such fracture zones would clearly be superior to theoretical considerations based on fracture study alone.

However, the spatial location of fracture zones does lead to delineation of potentially higher permeability zones. If the fracture zones are not sealed by mineralization or gouge, they may yield a preferred route for seepage at the mill site. In short, if controlled by fracture zones associated with lineaments, the seepage would be zoned linearly and be neither random nor occurring in all directions. Vertical migration of seepage would tend to be contained within the sandstone fractures because these do not continue through the underlying shales to the next lower sandstones.

## SEISMOTECTONICS

### INTRODUCTION

The Church Rock site is in a sparsely populated region where few seismic instruments exist and the record is short. An evaluation which combines local tectonic and paleotectonic information with seismic history is most effective under such circumstances. Where strong motion instrumental data is too sparse to define clear epicentral trends and clusters and where virtually no micro-seismal data exists, the problem of evaluating the distribution of variation in seismic potential must be approached tectonically.

Tectonic evidence must be used to sort earthquakes associated with first order tectonic features such as sub-block boundaries from earthquakes associated with intra-block processes. Intra-block processes induce earthquakes of lower magnitude which are more evenly distributed than earthquakes along sub-block boundaries (Smith and Sbar, 1974). Intra-block earthquakes in a region can sometimes be related to specific faults. Since smaller earthquakes do not often induce surface rupture, the relationship between seismic events and individual faults is not always apparent. It is often necessary to assign some intra-block earthquakes to a "random" class. This is necessary to account for the possibility of the occurrence of "unknown" earthquake source structures and does not imply that earthquakes occur without faulting.

The inverse of the foregoing case is true, however, in that known potential source structures in a region can be used to estimate the limiting size and location of intra-block earthquakes. Within a tectonically coherent region such as the Colorado Plateau, when estimates of maximum credible earthquakes from seismic history and from the evaluation of local structures can be resolved, the best possible estimates of seismic potential can be made. This method has the considerable advantage that maximum combined usefulness of two related but independent classes of information can be made in the case where information is sparse.

The site is situated on one of the intrablock features which might be hypothetically chosen as a source structure (the Pipeline Canyon lineament). A consideration of its relationship to the tectonics of the region, its seismogenic potential with respect to the regional seismic history, and to the seismogenic potential of other structures in the region provides a conservative means of defining upper limits of seismic design parameters at the site.

#### REGIONAL TECTONIC HISTORY: SUMMARY

All of the faults which shaped the late Cretaceous - early Tertiary history of the region are syndepositional with and no longer active as a result of the original tectonics of the Colorado Plateau (see page 9 ). The site is remote from the boundaries of the Colorado Plateau sub-block (Fig. 2). Surface stress measurements, mine studies, and focal plane solutions for instrumentally recorded earthquakes imply that the Colorado Plateau is in a state of east-west horizontal compression (Fig. 17). This agrees with plate tectonic theory for the region and explains the late Cenozoic coherency of the region which is located between two axes of spreading (Rio Grande rift and the Basin and Range spreading axis).

The site area is situated within an uplift block on a feature which is probably a minor fault related to the block margin. The Pipeline Canyon fault can therefore be interpreted as a third order kinematic element of a no longer active tectonic system. Its length and the relatively low magnitude of strain evident along its extent support this interpretation.

The seismic potential of the faults in the site region is the result of the modern regional stress field which may cause local reactivation of favorably oriented faults. The Pipeline Canyon fault is favorably oriented for reactivation with respect to the regional stresses.

#### SEISMIC POTENTIAL OF FAULTS IN THE SITE REGION

##### The Pipeline Canyon Lineament

The Pipeline Canyon lineament is approximately 15 miles long. If the entire length of the subsurface expression of the Pipeline Canyon fault is

1000000000

1000000000

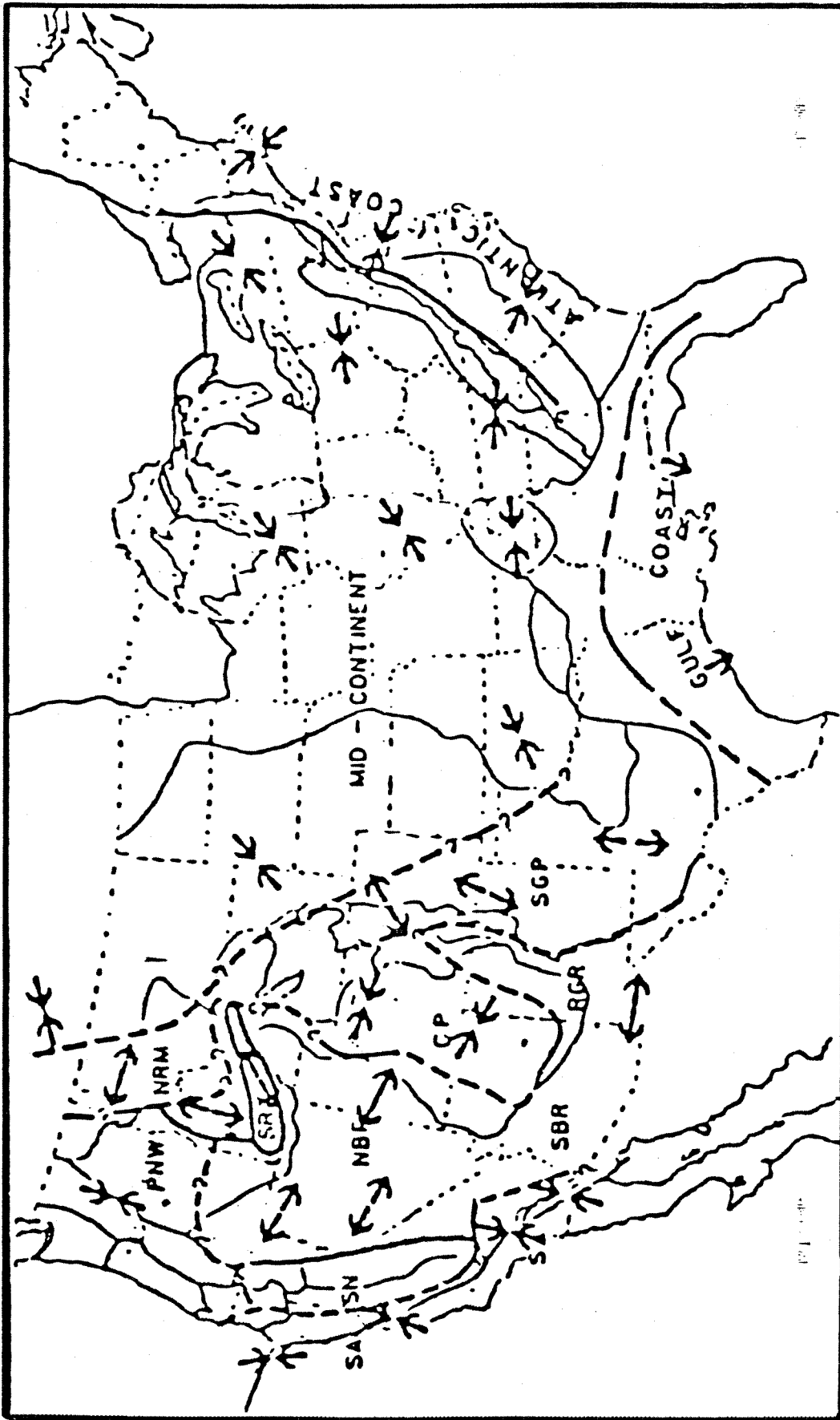


Figure 17. Map of maximum principle stress directions; stress provinces are indicated by thick lines (after Zoback and Zoback, 1980).

taken to be the length of a hypothetical fault, and if one half of that length is taken as a hypothetical surface rupture, the resultant hypothetical rupture length is 7.5 miles. This represents a conservative estimate of surface rupture length in the absence of historical surface rupture observations (Bonilla, 1967). This corresponds to a theoretical maximum credible Richter earthquake magnitude of 6.0 according to Bonilla's method. Since the site lies on the Pipeline Canyon lineament, the focal region of the theoretical maximum credible earthquake must hypothetically lie beneath the site at the average regional focal depth (6.25 miles).

### Seismic History of the Region

All of the large or moderate earthquakes in the region have occurred in the Rio Grande depression or in the Gila National Forest. The Gila earthquake was associated with the triple intersection of the Rio Grande rift, the major strike-slip fault zone known as Walker's Lane, and an apparent spreading ridge (the Texas lineament) which trends southeast from the Mogollon Region into Mexico. These are first-order regional tectonic features which form the southern and western boundaries of the Colorado Plateau sub-block. The second order tectonic features associated with the southeastern Colorado Plateau region are northeasterly trending zones of seismicity, faulting, and geophysical and photo-geologic lineaments. These zones define regions of maximum seismicity where they intersect the Rio Grande rift and connect major late Cenozoic volcanic centers (Sanford *et al.*, 1978). These features may represent transform faults associated with the Texas lineament (William Muehlburger, 1979, personal communication; Gibbons, 1979). All of these structures identified to date lie to the southeast of the site. The present northern terminus of the Texas lineament now lies far to the southeast of the site, implying that no faulting related to transform activity on that ridge can be expected in the site area in the foreseeable future. Only very small, shallowly focused earthquakes on pre-existing faults, resulting from tractional stresses transmitted across the boundaries of the block, are likely in the site area. On the basis of these tectonic considerations, the seismic history pertinent to the site is that of the south central Colorado Plateau region only.

Various assessments of south-central Colorado Plateau seismic history have been generated. The most recent, and the one using the most modern methods is inapplicable to the site area. This study (Newton, *et al.*,) makes use of microseismal data from a net at Los Alamos, New Mexico and uses modern statistical techniques of McGuire (1977). Its resolving power diminishes rapidly outside the Los Alamos net and assumptions are made about regional recurrence intervals that are clearly unrelated to the site area. In one case the Los Alamos study makes use of a theoretical maximum recurrence interval to calculate maximum credible earthquakes which approach Richter magnitude 7. Regional seismic history clearly demonstrates that the assumed value of recurrence is inappropriate. Using the same regional seismic history and recurrences calculated from strong motion data along the Rio Grande rift (Sanford, *et al.*, 1972, 1978), a much more reasonable Richter magnitude of 5.6 was the result. The authors (Newton, *et al.*,) stress in several places in their paper that no design conclusions can be drawn outside their microseismal net.

Although an earthquake of Richter magnitude 5.6 is more reasonable than a Richter magnitude earthquake of 7 for the site region, it may represent a recurrence interval that is inappropriate to the site. Sanford *et al.*, (1972) has developed the most widely accepted earthquake history of the Rio Grande rift. Both the data distribution used by Sanford and his interpretive intent were to characterize the recurrence relationships on structures along the rift. Inasmuch as the rift comprises one of the sub-block boundaries of the Colorado Plateau, seismicity along such a feature should differ substantially from that of intra-block areas (Smith and Sbar, 1974). Lower energy release levels and longer periods between earthquakes should be characteristic of intra-block areas relative to their nearest boundaries.

The above reasoning accounts for Sanford's willingness to predict maximum credible events near 5.0 for areas west of the rift (Bokum Groundwater Discharge Plan, 1979). Short facility life with respect to long recurrence intervals in a large area of relatively low energy release distributes the probability of large earthquakes toward very small values.

With respect to the Church Rock site, these observations must be tempered by the location of the site on a zone which implies the existence of an ancient basement fault, not occurring as a fault in the rocks of interest at the site. Reconnaissance of the Pleistocene sediments in the Puerco River Valley in the site vicinity showed no identifiable offsets. At Location 41 a shear zone which is part of the Fort Wingate lineament is exposed in the siltstones of the upper Mancos in the stream bed. A thorough study of the Pleistocene sediments exposed in the stream where they overlie the shear zone revealed no offsets implying that this feature has not been reactivated.

The absolute or stratigraphic ages of the soils and sediments of the Puerco Valley have not been firmly established. The discovery of a mid-Pleistocene fossil horse from the silty sediments near Location 41 implies that the base of the Pleistocene sedimentary sequence is at least pre late Pleistocene (Barry Keyes, 1980, personal communication).

The absence of instrumentally recorded seismic activity associated with the observed structural zones at the site and the physical evidence cited above strongly imply that no reactivation of faulting associated with the Pipeline Canyon lineament as a result of modern tectonic stresses has occurred in the site area. This implies that the risk of surface rupture at the site is not significantly higher than the surrounding terrain which is very low. Another strong implication is that the 6.0 maximum credible Richter magnitude earthquake calculated on the basis of a 7.5 mile surface rupture using the Bonilla method is overly conservative. In an area where information is sparse, values based on qualitative weighing of factors is sometimes necessary. Among Richter magnitude values in use in the region (Sanford's low 5's and LASL's 5.6's) and theoretical maximum values based on the presence of the Pipeline Canyon lineament (6.0), the short life of the facility relative to all estimated recurrances argues for a moderately low value for any design basis earthquake for this facility. It is recommended that a design basis earthquake of Richter magnitude 5.4 be employed in any stability considerations at the Church Rock site.

# APPENDIX A

## FRACTURE STUDY ANALYSIS

### Discussion

- Figures A-1 through A-15      Pi diagram: lower hemisphere equal area projection
- Figures A-16 through A-22   - Fracture spacing analysis, histograms
- Tables A-1 through A-5       - Summary of fracture data



## FRACTURE STUDY ANALYSIS

The fracture study at the site area, conducted in conjunction with the structural study, was designed to establish the overall fracture geometry in the area, and, to quantify as much as possible, the fracture density of the lithologic units which directly underlie the tailings pond at the Church Rock facility. Each task was conducted separately and the method of data collection varied for each.

### FRACTURE GEOMETRY: METHOD AND PROCEDURE

To determine the regional fracture pattern, sampling areas were chosen which avoided linear elements or changes in structural attitude. Specific sites were selected after a brief reconnaissance to determine the shape and extent of the outcrop, presence of representative fractures, proximity to the tailings pond, and lithologic unit. For this task, sampling was restricted to the sandstone outcrops of the lower and upper Gallup Sandstone and the Dilco Coal, both members of the Crevasse Canyon Formation. Data was collected from fifteen locations (Sites 1-15, Map A-1), nine along the Pipeline Canyon lineament and six around Ram Mesa, a major topographic feature which lies south and west of the tailings pond and southeast of the Pipeline Canyon linear which changes direction (north) at Ram Mesa. Thirteen locations were sampled from the lower and upper Gallup Sandstone and two were sampled from the Dilco Coal Member (Figs. A-1 - A-15).

Fractures were three-dimensional features; therefore, to accurately define the overall fracture geometry, circular sampling patterns yield the most complete set of data. Outcrops which were ideally suited for this kind of sampling were not available in the study area; consequently, sites had to be selected which continued around the mouth or head of the canyons along the mesas.

The length of each sampling site was determined by the distance required to measure 100 consecutive fractures which occurred within reasonable distance of each other. Two feet was the minimum fracture length allowed for sampling. One hundred data points would allow an accurate picture of the major fracture trends (see p. 53).

The strike and dip of each fracture was taken using a Brunton pocket transit. Fracture fill, estimated length, opening, and planarity were also recorded.

#### FRACTURE SPACING: METHOD AND PROCEDURE

In the second phase of the fracture study, a second set of data was gathered to determine fracture density in the site area. Sample traverses perpendicular to the traces of the three major structural features were carried out where cover conditions and land access arrangements permitted (Sites 16-32, Map A-1). For this task, sites were chosen which permitted data collection along a straight line (rather than a circular pattern) perpendicular to a structural trend. The number of fractures per ten foot interval was recorded over an undesignated distance. The length of the traverse varied due to availability of outcrop, natural obstacles, and rubble zones.

Data collection differed slightly depending upon which type of structural feature was being sampled. For traverses perpendicular to the two major structural features (the Pipeline Canyon and Fort Wingate lineaments, and associated monoclinial folds; Sites 16-26, Map A-1) each type of fracture present was counted separately: vertical fractures, high angle fractures ( $70^{\circ}$ ), and low angle fractures ( $30^{\circ}$ - $40^{\circ}$ ). Three low angle fractures were counted over a total of eleven sampling locations. Fracture types were not distinguished for locations sampled along the Pinedale monocline (for a discussion, see text, Fracture Patterns, and Fig. 10). For this task all lithologic units in the site area, up to and including, the Point Lookout Sandstone were sampled.

#### DATA ANALYSIS

##### Fracture Geometry

A Tektronix 4052 was used to generate pi diagrams for each of the fifteen locations. Pi diagrams are generated by plotting the pole of a measured plane (using the strike and dip) on an equal area lower hemisphere projection. A greater amount of accuracy is assured by using the simpler pi diagram than by using a beta diagram which plots the actual measured plane. An equal area

projection is preferable to a stereographic (or equiangular) projection because it does not distort equal concentrations of points, although shapes of plotted concentrations will be distorted. On a stereographic projection equal concentrations of points will appear as unequal concentrations. Equal area projections are commonly used for plotting distributions of fractures and will form a pattern diagnostic of the structure (in this case the regional fracture pattern). Also, most counting nets used for contouring are designed for use with an equal area net.

Contouring was done using a Kalsbeek counting net, one of the many kinds of counting nets available, to construct a point diagram. This particular net is subdivided into triangles. Any six contiguous triangles form a hexagon which is equal to 1% of the total area. With the Kalsbeek net there is a fixed relationship between the total number of points and the counted density (except for a small discrepancy at the ends of the spokes). After the point diagrams were completed, contours of equal density were drawn. If 100 data points are used, each number on the point diagram equals the actual percent of the total.

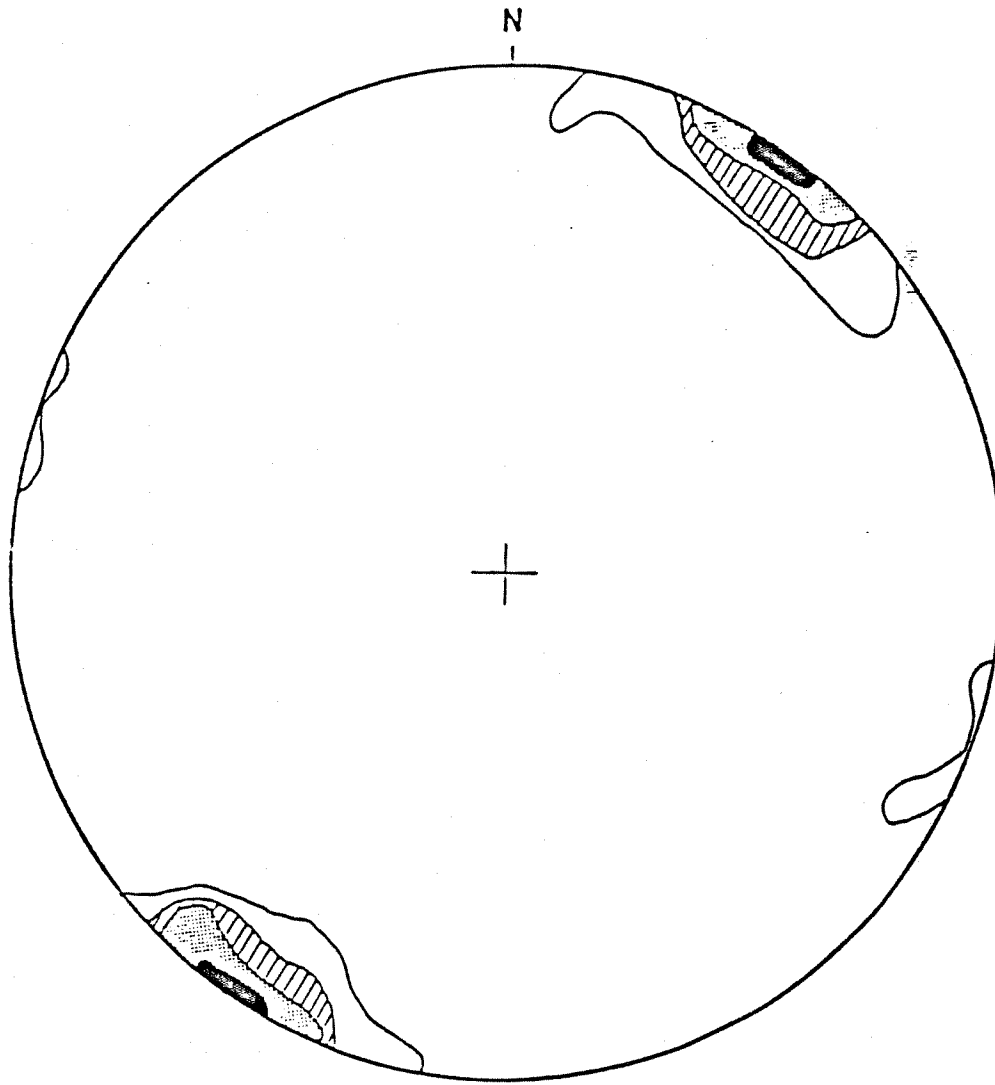
The results of this analysis are presented in Figs. A-1 through A-15. Contour intervals were designated for each site individually to more accurately present variations at each location. The pi diagrams confirmed field observations that the regional fracture pattern is made up of two sets of fractures which strike north-northeast and west-northwest.

### Fracture Spacing

Histograms were generated for each of the seventeen sites sampled (Figs. A-16 - A-22). Linear regressions were performed for each set of data and confirmed that fracture spacing is regular. The three types of fractures were plotted separately on each graph; vertical fractures and high angle fractures did not generally occur within the same intervals.

Site 24 was the longest location sampled (5630 ft); the line of traverse both paralleled and was perpendicular to the Pipeline Canyon lineament and the Pinedale monocline (Map A-1). Five linear subsets (24a-24e) were defined during the analysis to determine if the curvilinearity of the traverse had a significant effect on the analysis. Overall results did not differ significantly (Tables

A-1 and A-2). The results of the analysis are presented in Tables A-1 through A-4. Table A-5 summarizes the frequency of occurrence of fractures per 10 feet for each site. Zero and one are the most frequently occurring number of fractures per 10 feet (see text for discussion).



LOCATION: MAP A-1 SITE 1

STRATIGRAPHIC UNIT: Upper Gallup Sandstone

MEAN THICKNESS: 20 feet

SAMPLE SIZE: 97

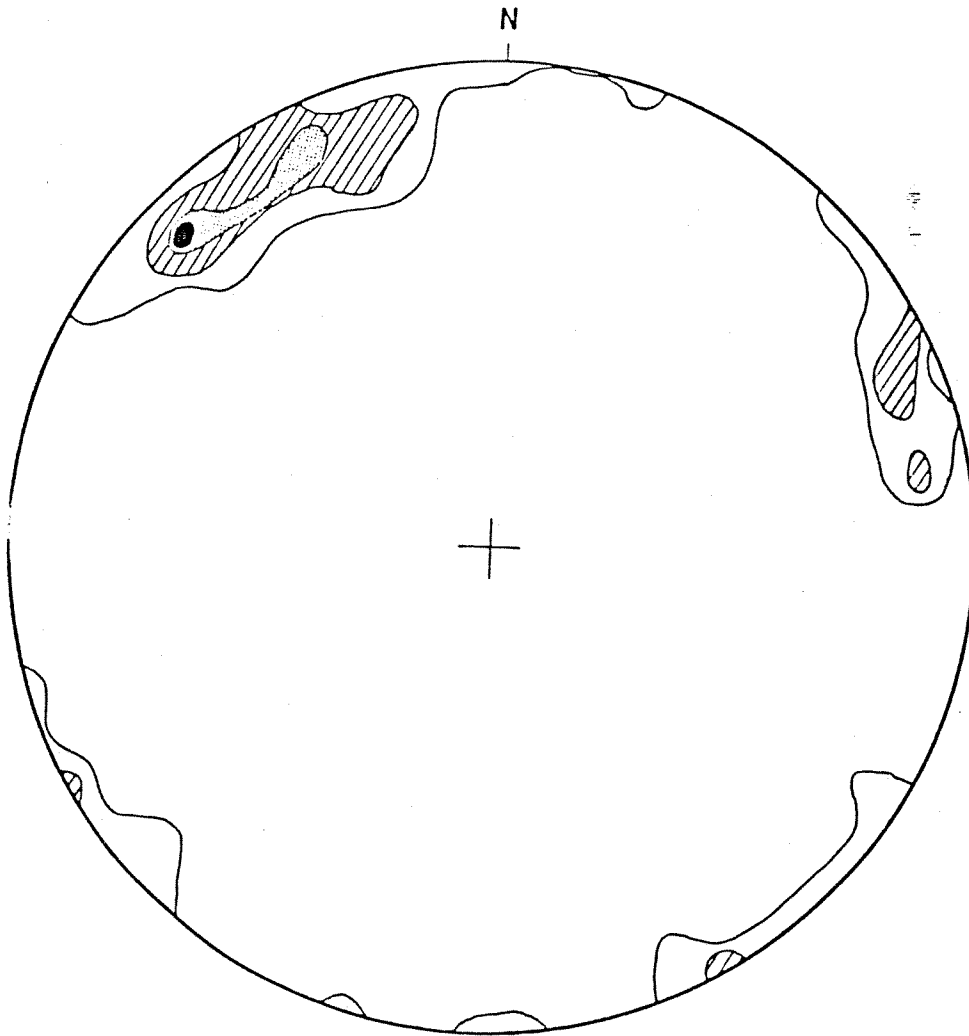
FRACTURE FILL (IF PRESENT): limonite mineralization

ASSOCIATED FEATURES: Ram Mesa

CONTOUR INTERVAL: 4-7-11-15%      MAXIMUM PERCENT: 17%

PI DIAGRAM: LOWER HEMISPHERE EQUAL AREA PROJECTION

Figure A-1



LOCATION: MAP A-1 SITE 2

STRATIGRAPHIC UNIT: Upper Gallup Sandstone

MEAN THICKNESS: 30 feet

SAMPLE SIZE: 100

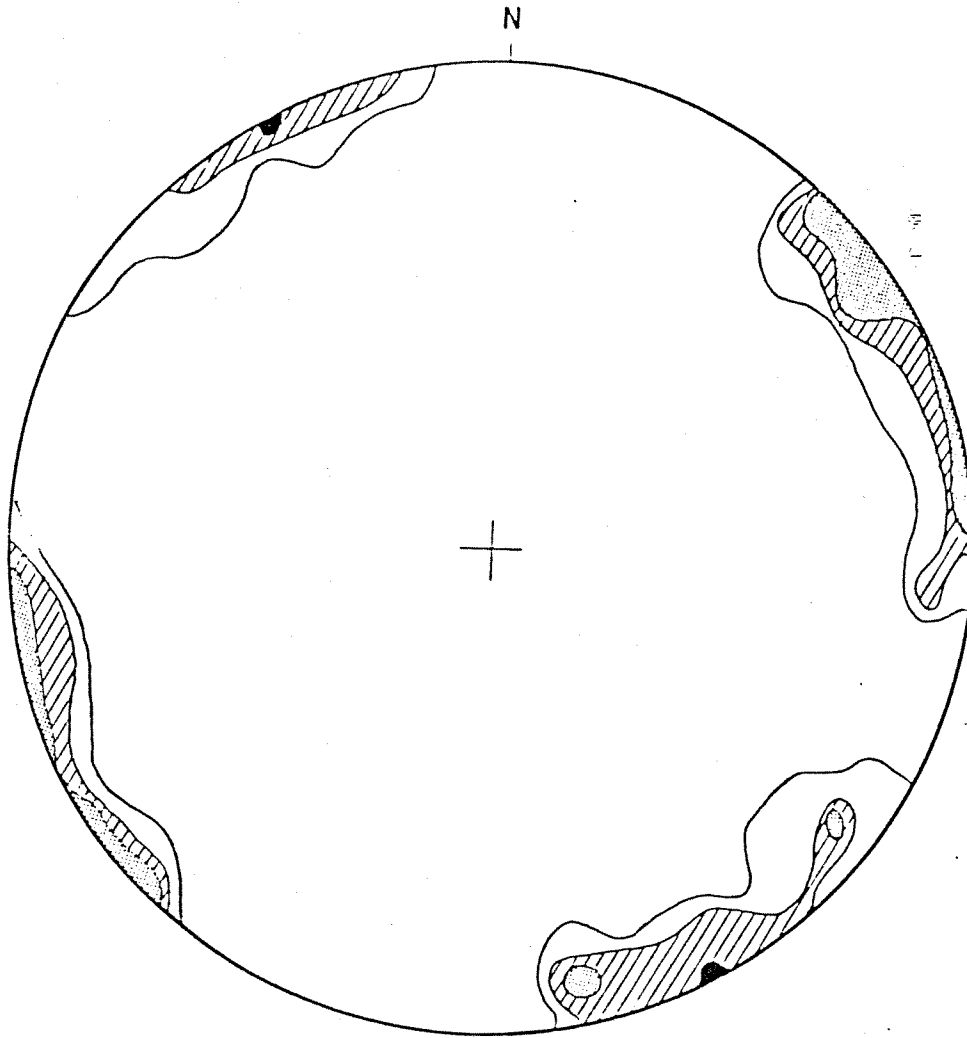
FRACTURE FILL (IF PRESENT):

ASSOCIATED FEATURES: Pipeline Canyon lineament

CONTOUR INTERVAL: 5-7-8-10%      MAXIMUM PERCENT: 10%

PI DIAGRAM: LOWER HEMISPHERE EQUAL AREA PROJECTION

Figure A-2



LOCATION: MAP A-1 SITE 3

STRATIGRAPHIC UNIT: Lower Gallup Sandstone

MEAN THICKNESS: 40 feet

SAMPLE SIZE: 100

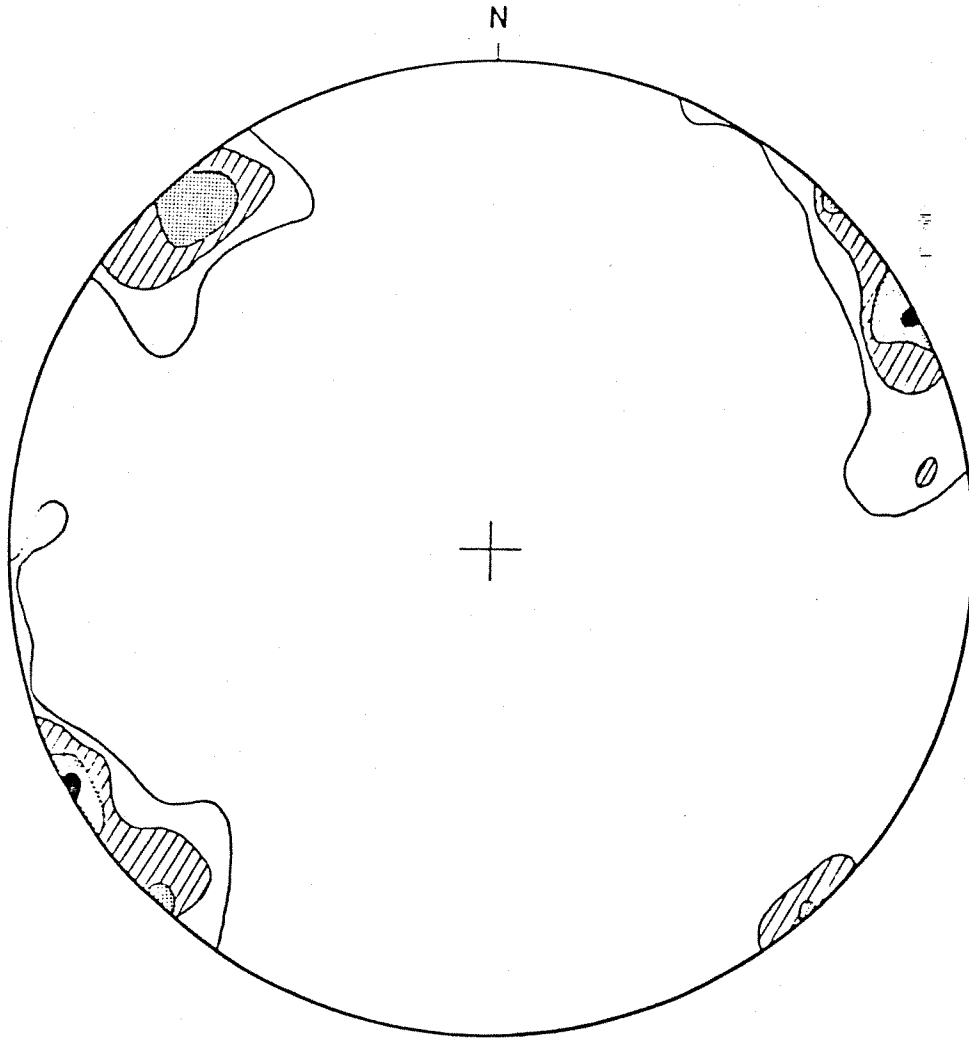
FRACTURE FILL (IF PRESENT):

ASSOCIATED FEATURES: Pipeline Canyon lineament

CONTOUR INTERVAL: 3-5-7-9%      MAXIMUM PERCENT: 9%

PI DIAGRAM: LOWER HEMISPHERE EQUAL AREA PROJECTION

Figure A-3



LOCATION: MAP A-1 SITE 4

STRATIGRAPHIC UNIT: Lower Gallup Sandstone

MEAN THICKNESS: 25 feet

SAMPLE SIZE: 100

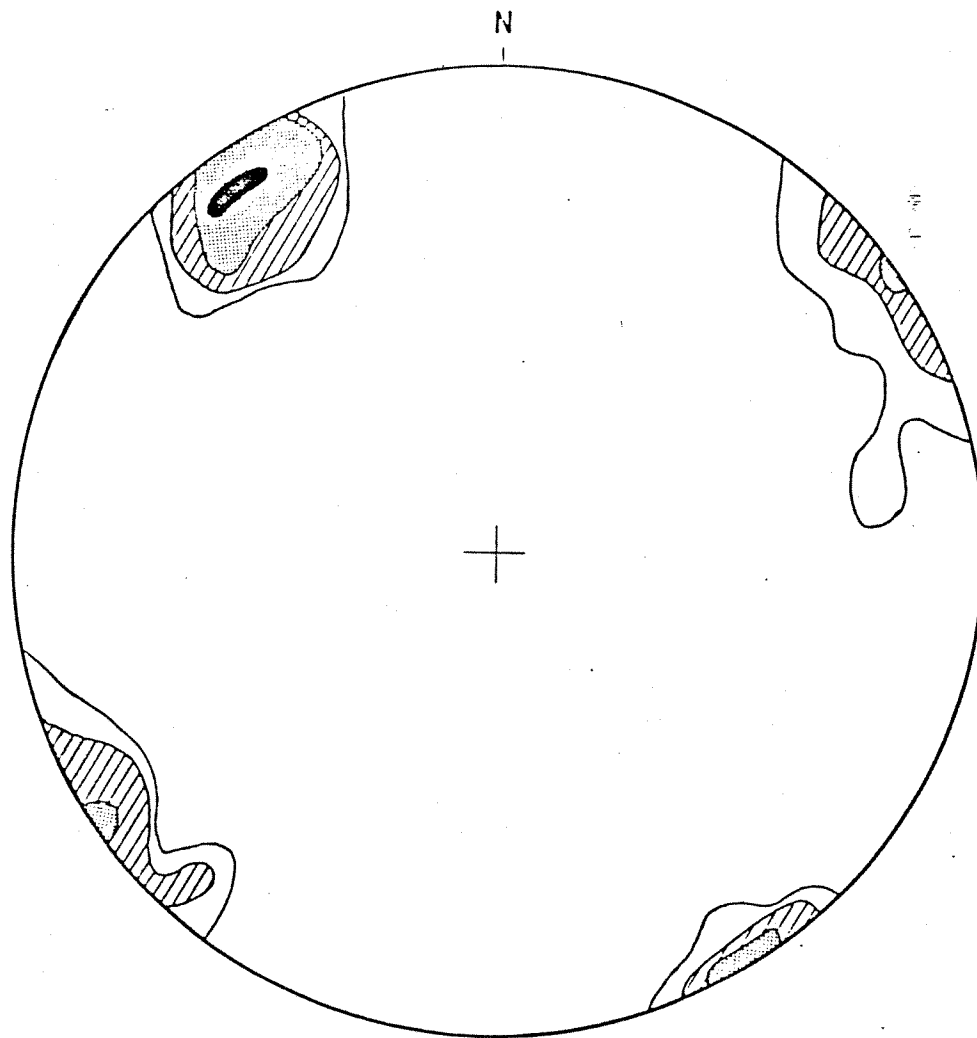
FRACTURE FILL (IF PRESENT): limonite mineralization, sand

ASSOCIATED FEATURES: Pipeline Canyon lineament

CONTOUR INTERVAL: 4-7-10-13%      MAXIMUM PERCENT: 14%

PI DIAGRAM: LOWER HEMISPHERE EQUAL AREA PROJECTION

Figure A-4



LOCATION: MAP A-1 SITE 5

STRATIGRAPHIC UNIT: Lower Gallup Sandstone

MEAN THICKNESS: 50 feet

SAMPLE SIZE: 100

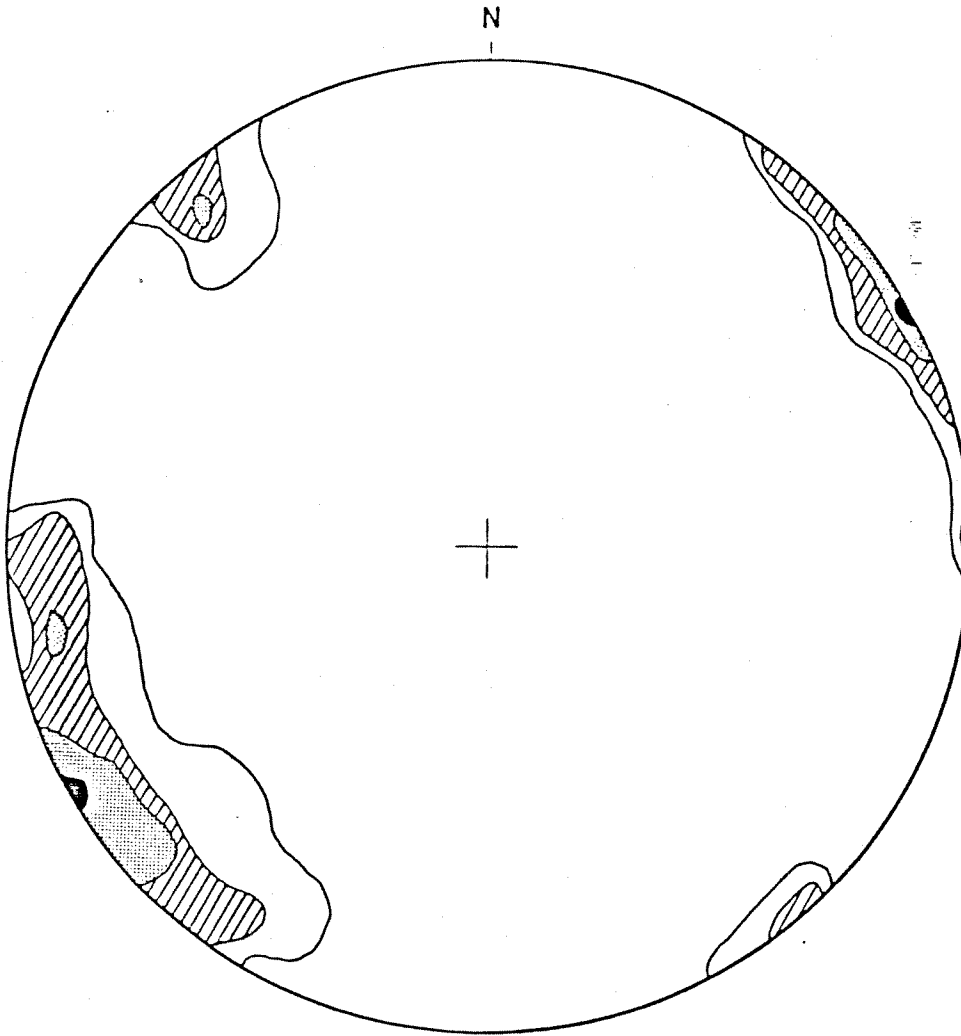
FRACTURE FILL (IF PRESENT):

ASSOCIATED FEATURES: Pipeline Canyon lineament

CONTOUR INTERVAL: 3-6-10-20%      MAXIMUM PERCENT: 24%

PI DIAGRAM: LOWER HEMISPHERE EQUAL AREA PROJECTION

Figure A-5



LOCATION: MAP A-1 SITE 6

STRATIGRAPHIC UNIT: Dilco Coal

MEAN THICKNESS: 25 feet

SAMPLE SIZE: 100

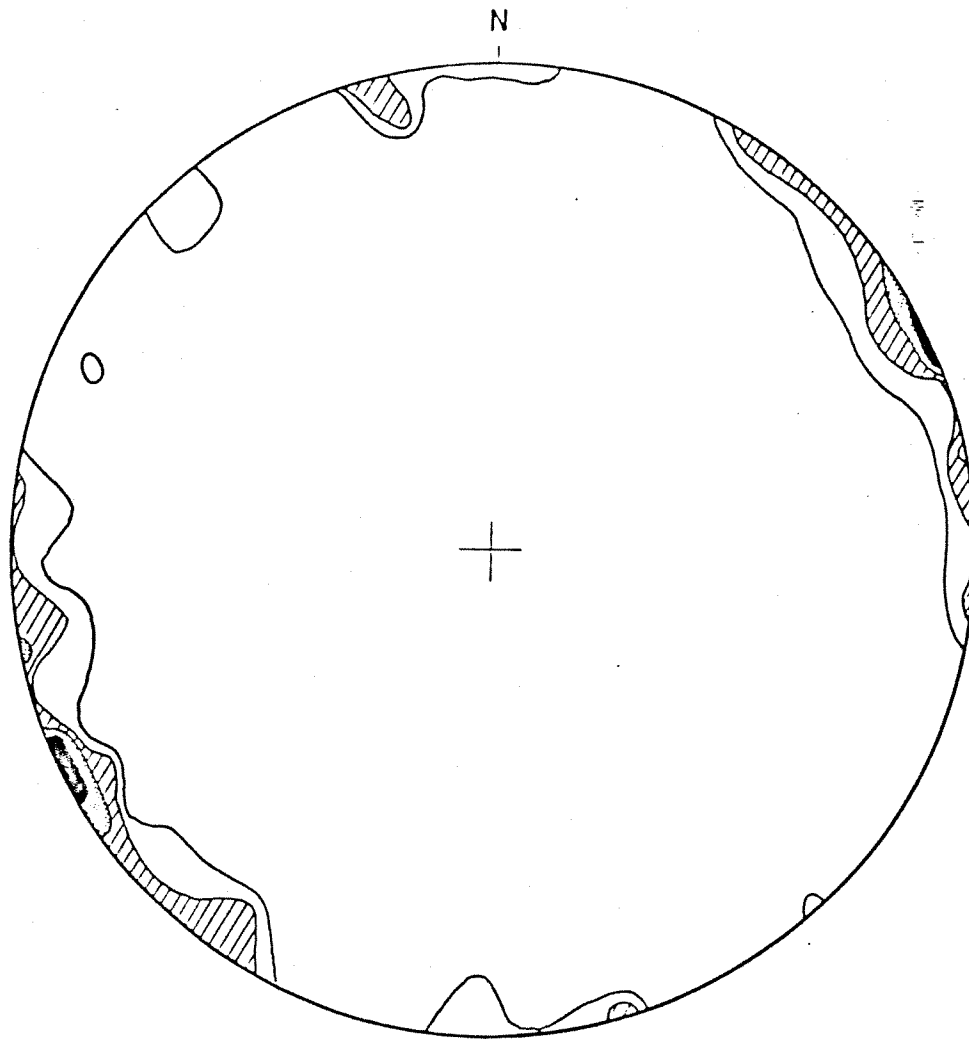
FRACTURE FILL (IF PRESENT): sand, rubble

ASSOCIATED FEATURES: Pipeline Canyon lineament

CONTOUR INTERVAL: 3-6-9-12%      MAXIMUM PERCENT: 13%

PI DIAGRAM: LOWER HEMISPHERE EQUAL AREA PROJECTION

Figure A-6



LOCATION: MAP A-1 SITE 7

STRATIGRAPHIC UNIT: Upper Gallup Sandstone

MEAN THICKNESS: 6 feet

SAMPLE SIZE: 100

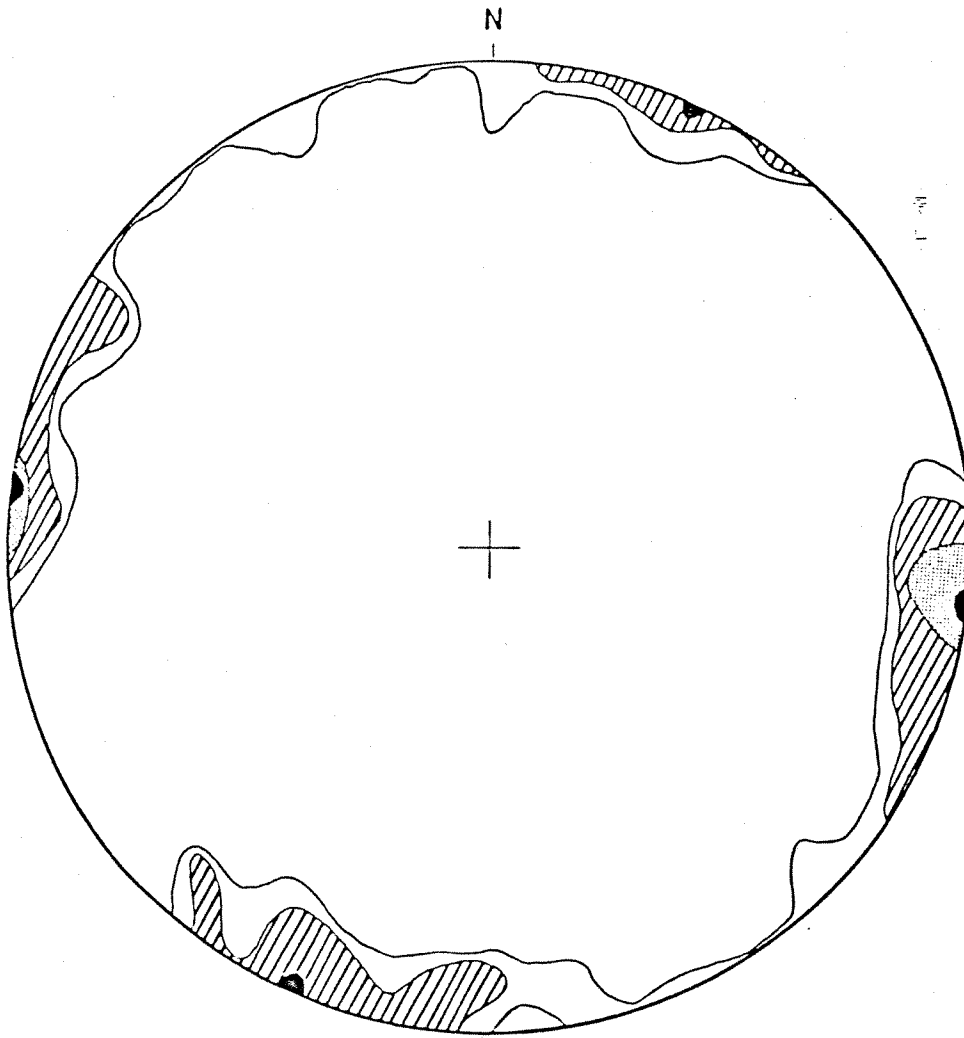
FRACTURE FILL (IF PRESENT): sand, rubble

ASSOCIATED FEATURES: Pipeline Canyon lineament

CONTOUR INTERVAL: 4-7-10-13%      MAXIMUM PERCENT: 14%

PI DIAGRAM: LOWER HEMISPHERE EQUAL AREA PROJECTION

Figure A-7



LOCATION: MAP A-1 SITE 8

STRATIGRAPHIC UNIT: Upper Gallup Sandstone

MEAN THICKNESS: 4 feet

SAMPLE SIZE: 100

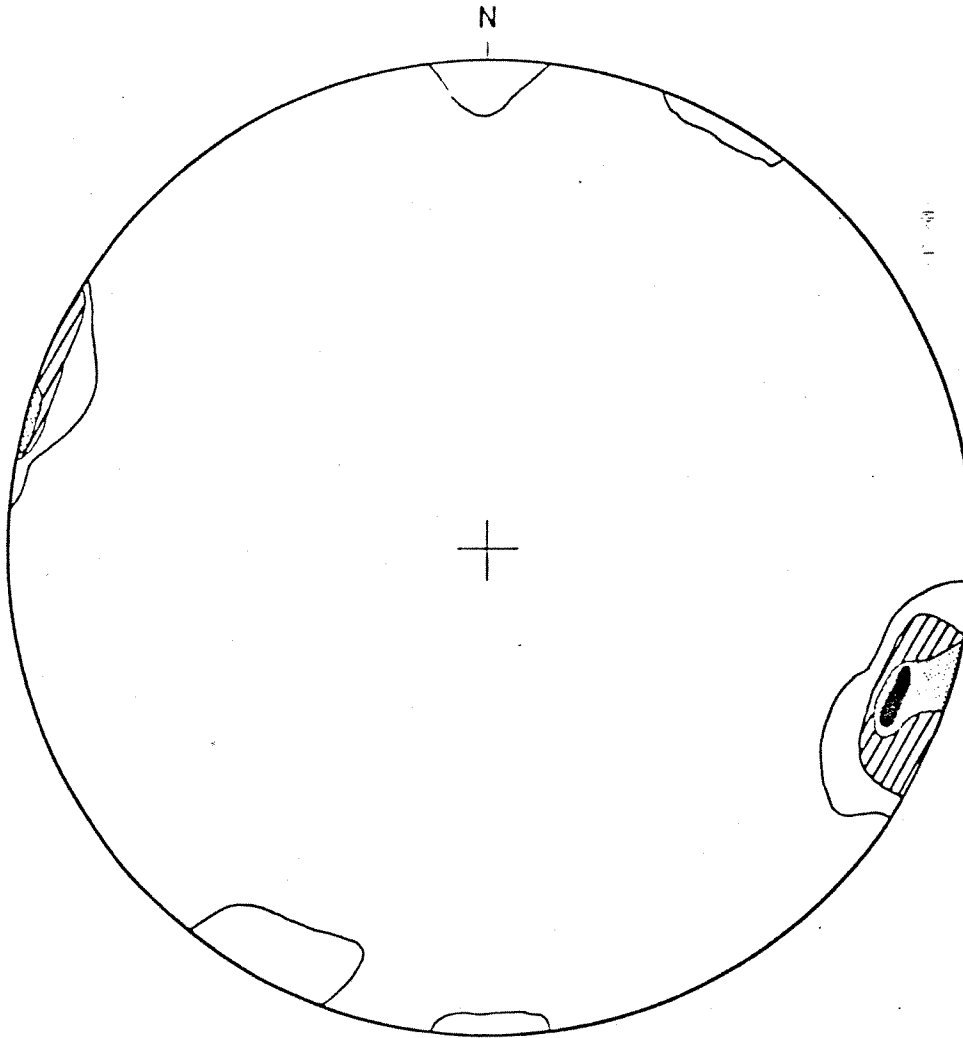
FRACTURE FILL (IF PRESENT): sand

ASSOCIATED FEATURES: Ram Mesa

CONTOUR INTERVAL: 3-5-9-12%      MAXIMUM PERCENT: 14%

PI DIAGRAM: LOWER HEMISPHERE EQUAL AREA PROJECTION

Figure A-8



LOCATION: MAP A-1 SITE 9

STRATIGRAPHIC UNIT: Upper Gallup Sandstone

MEAN THICKNESS: 75 feet

SAMPLE SIZE: 100

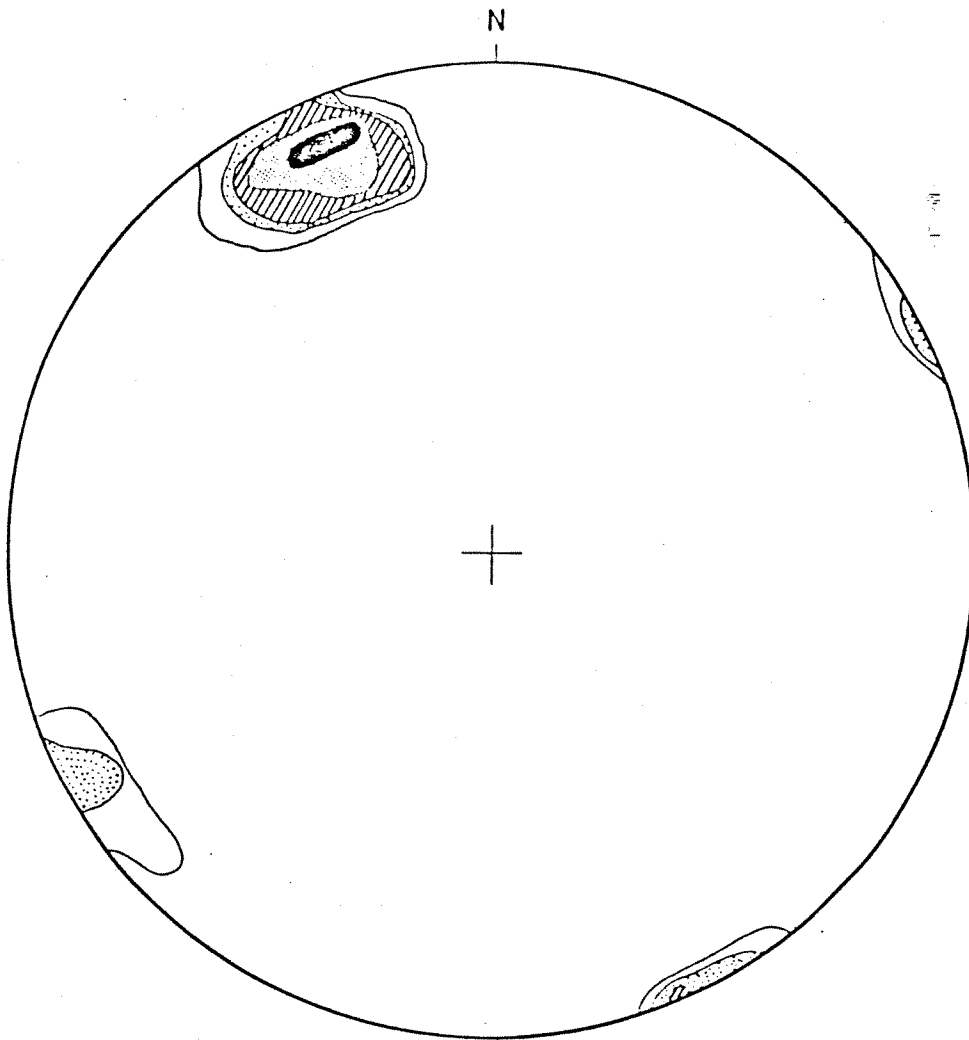
FRACTURE FILL (IF PRESENT): limonite mineralization

ASSOCIATED FEATURES: Ram Mesa

CONTOUR INTERVAL: 5-10-16-20%      MAXIMUM PERCENT: 21%

PI DIAGRAM: LOWER HEMISPHERE EQUAL AREA PROJECTION

Figure A-9



LOCATION: MAP A-1 SITE 10

STRATIGRAPHIC UNIT: Upper Gallup Sandstone

MEAN THICKNESS: 30 feet

SAMPLE SIZE: 100

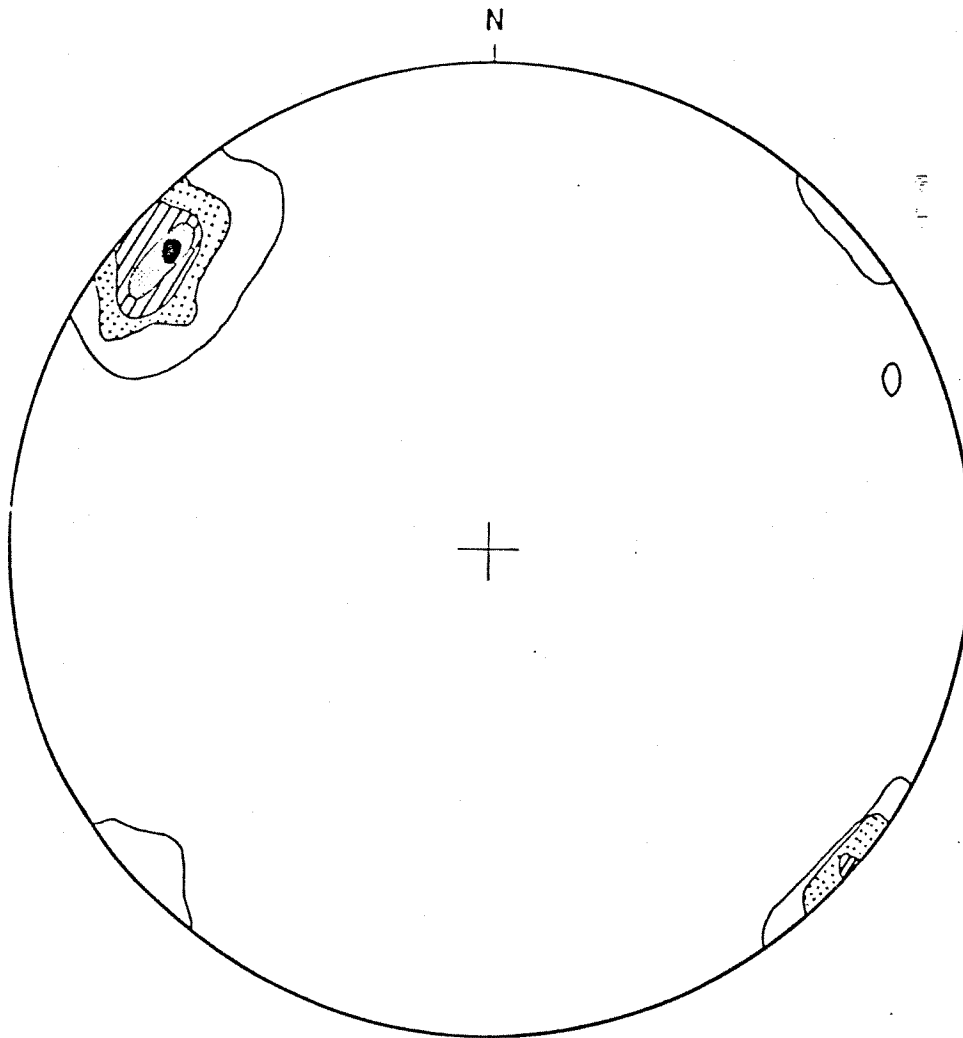
FRACTURE FILL (IF PRESENT):

ASSOCIATED FEATURES: Pipeline Canyon lineament

CONTOUR INTERVAL: 4-6-10-15-25% MAXIMUM PERCENT: 27%

PI DIAGRAM: LOWER HEMISPHERE EQUAL AREA PROJECTION

Figure A-10



LOCATION: MAP A-1 SITE 11

STRATIGRAPHIC UNIT: Lower Gallup Sandstone

MEAN THICKNESS: 50 feet

SAMPLE SIZE: 100

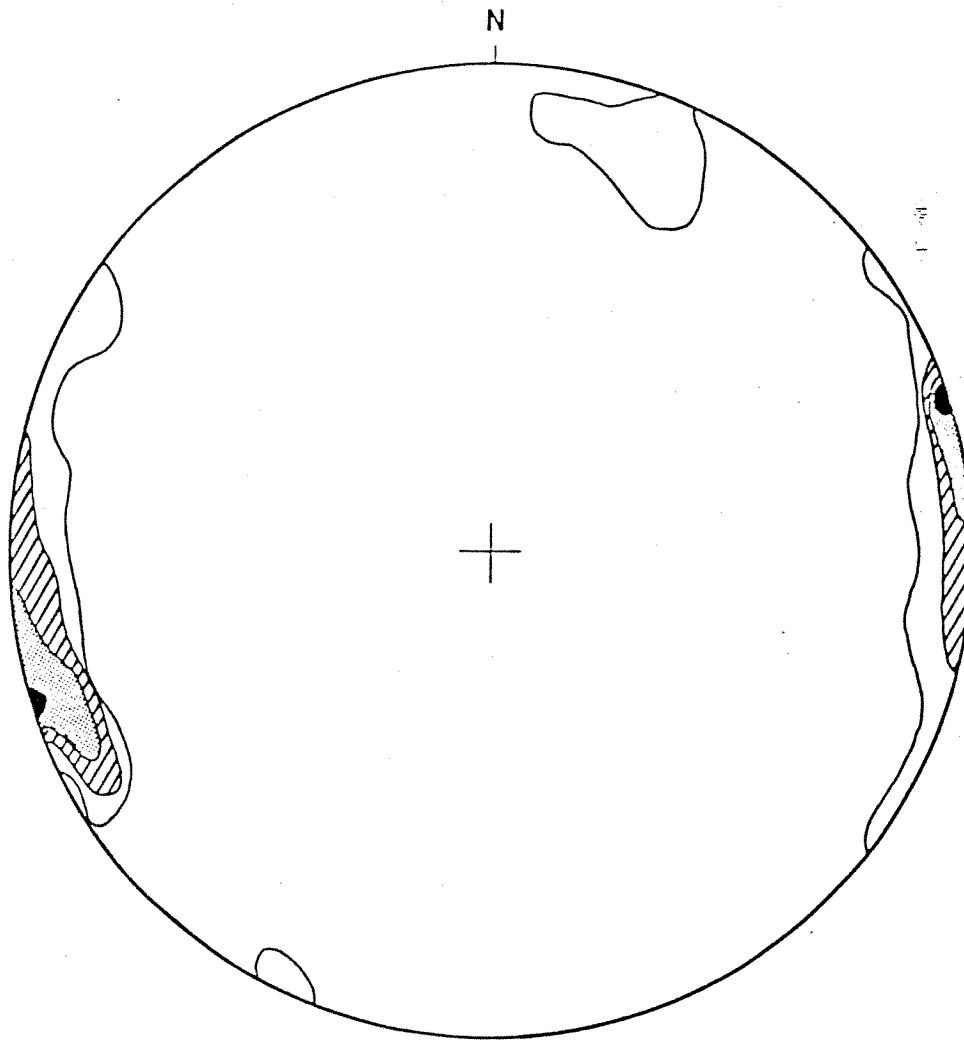
FRACTURE FILL (IF PRESENT):

ASSOCIATED FEATURES: Pipeline Canyon lineament

CONTOUR INTERVAL: 5-13-17-25% MAXIMUM PERCENT: 33%

PI DIAGRAM: LOWER HEMISPHERE EQUAL AREA PROJECTION

Figure A-11



LOCATION: MAP A-1 SITE 12

STRATIGRAPHIC UNIT: Upper Gallup Sandstone

MEAN THICKNESS: 30 feet

SAMPLE SIZE: 100

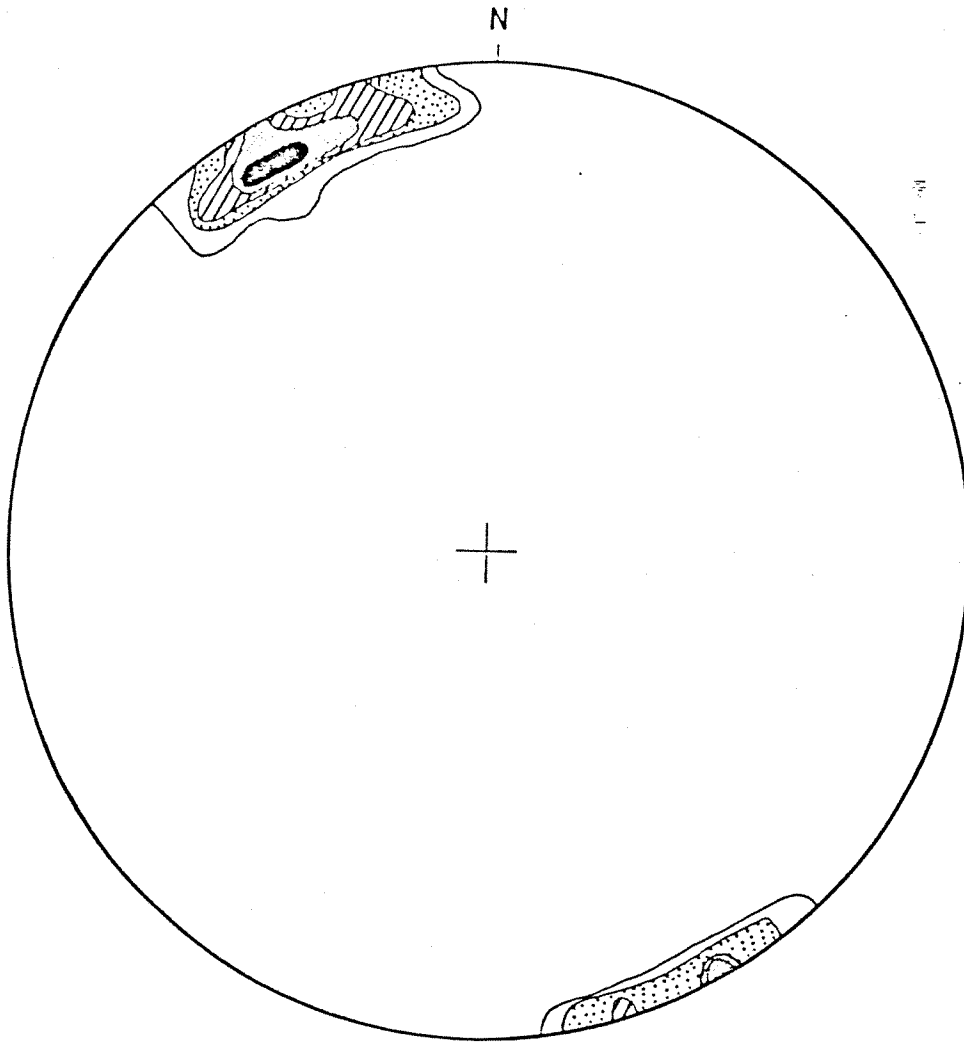
FRACTURE FILL (IF PRESENT):

ASSOCIATED FEATURES: Ram Mesa

CONTOUR INTERVAL: 4-7-10-14%      MAXIMUM PERCENT: 14%

PI DIAGRAM: LOWER HEMISPHERE EQUAL AREA PROJECTION

Figure A-12



LOCATION: MAP A-1 SITE 13

STRATIGRAPHIC UNIT: Upper Gallup Sandstone

MEAN THICKNESS: 15 feet

SAMPLE SIZE: 100

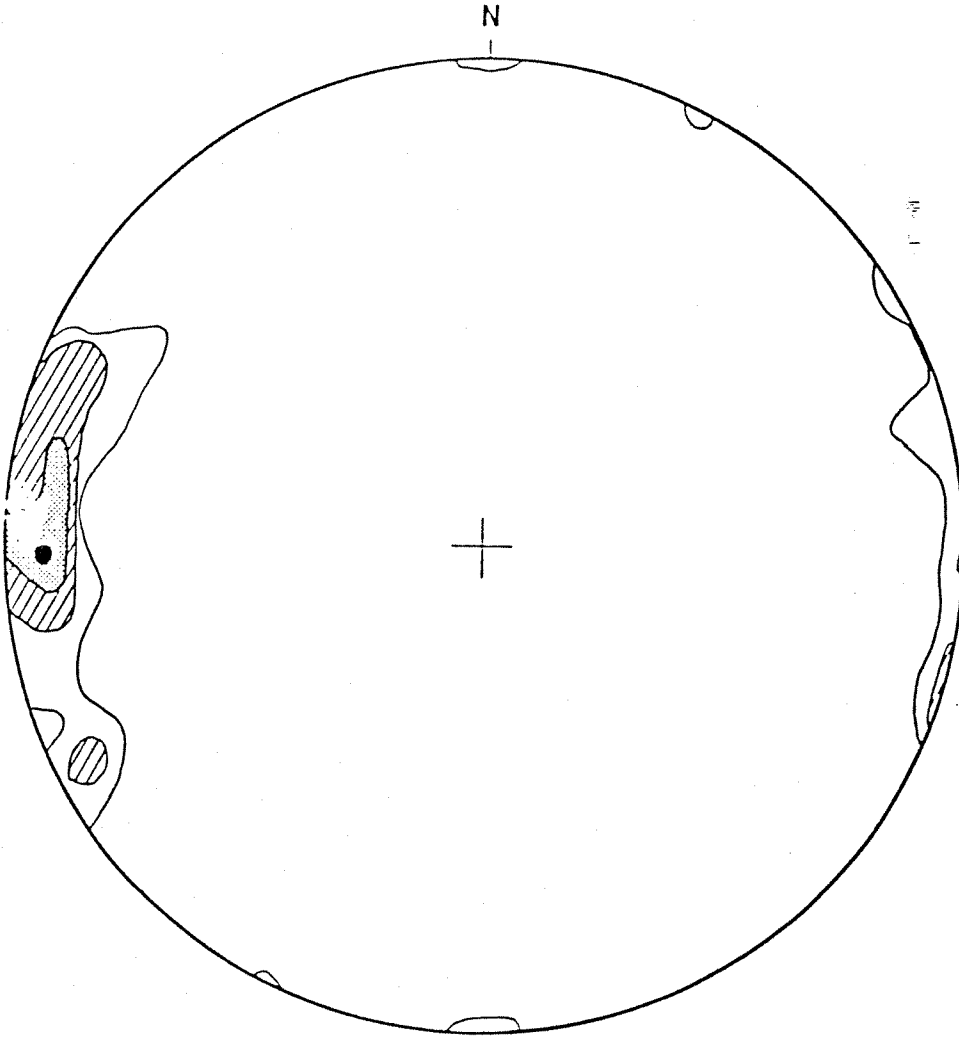
FRACTURE FILL (IF PRESENT): limonite mineralization, gypsum

ASSOCIATED FEATURES: Ram Mesa

CONTOUR INTERVAL: 5-12-17-25-30% MAXIMUM PERCENT: 31%

PI DIAGRAM: LOWER HEMISPHERE EQUAL AREA PROJECTION

Figure A-13



LOCATION: MAP A-1 SITE 14

STRATIGRAPHIC UNIT: Dilco Coal

MEAN THICKNESS: 5 feet

SAMPLE SIZE: 100

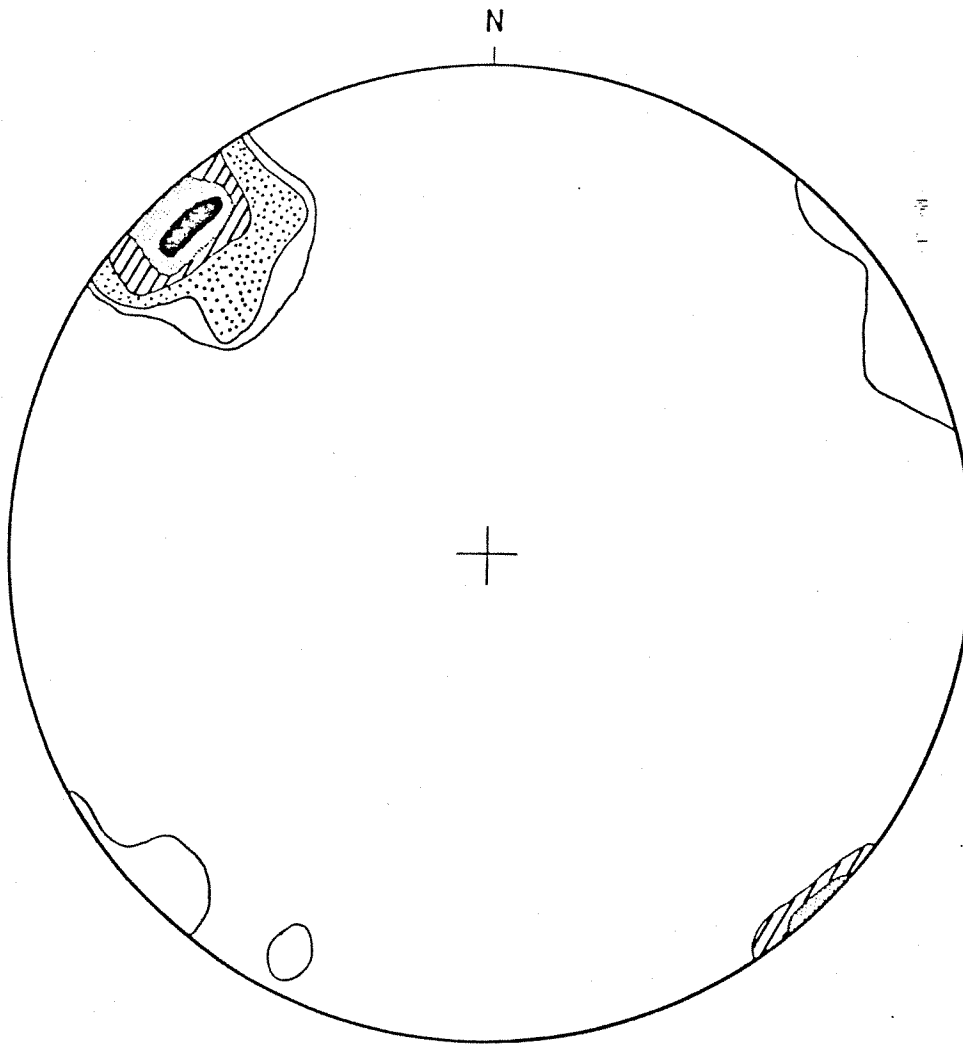
FRACTURE FILL (IF PRESENT): iron concretions

ASSOCIATED FEATURES: Ram Mesa

CONTOUR INTERVAL: 4-7-11-15%      MAXIMUM PERCENT: 16%

PI DIAGRAM: LOWER HEMISPHERE EQUAL AREA PROJECTION

Figure A-14



LOCATION: MAP A-1 SITE 15

STRATIGRAPHIC UNIT: Lower Gallup Sandstone

MEAN THICKNESS: 35 feet

SAMPLE SIZE: 100

FRACTURE FILL (IF PRESENT):

ASSOCIATED FEATURES: Pipeline Canyon lineament

CONTOUR INTERVAL: 4-6-11-16-21% MAXIMUM PERCENT: 25%

PI DIAGRAM: LOWER HEMISPHERE EQUAL AREA PROJECTION

Figure A-15

TABLE A-1. Summary of Fracture Data for All Fractures

Site	Stratigraphic Unit	Thickness (feet)	Length of Traverse (feet)	Total Fractures	Ave. No. Fractures/10 ft	Range
16	Kp1	20-30	640	54	0.9	0-5
17	Kp1	20-30	670	79	1.2	0-4
18	Kcd	10-15	520	0	---	---
19	Kcd	10-20	640	13	0.2	0-2
20	Kcd	10-25	780	33	0.4	0-2
21	Kg1	30-40	520	107	2.1	0-10
22	Kg1	20-40	1500	111	0.8	0-4
23	Kp1	10-25	230	192	0.9	0-4
24	Kp1	20-40	5630	395	0.7	0-4
24a	Kp1	20-40	250	29	1.3	0-3
24b	Kp1	20-40	700	73	1.1	0-4
24c	Kp1	20-40	750	55	0.7	0-4
24d	Kp1	20-40	1100	68	0.6	0-3
24e	Kp1	20-40	2830	170	0.6	0-4
25	Kcd	10-15	1340	187	1.4	0-6
26	Kcdc	10-15	1160	54	0.5	0-2
27	Kp1	10-20	490	120	2.4	0-9
28	Kcd	2-25	150	31	2.1	0-4
29	Kcd	15	970	272	2.8	0-9
30	Kcg	10-30	440	122	3.8	0-7
31	Kgu	30-40	720	92	1.3	0-5
32	Kgu	50-70	1080	123	1.4	0-4

TABLE A-2. Summary of Fracture Data for Vertical Fractures

Site	Stratigraphic Unit	Thickness (feet)	Length of Traverse (feet)	Total Fractures	Ave. No. Fractures/10 ft	Range
16	Kp1	20-30	640	34	0.6	0-5
17	Kp1	20-30	670	65	1.0	0-4
18	Kcd	10-15	520	0	---	---
19	Kcd	10-20	640	8	0.4	0-1
20	Kcd	10-25	780	27	0.4	0-2
21	Kg1	30-40	520	88	2.1	0-10
22	Kg1	20-40	1500	108	0.7	0-4
23	Kp1	10-25	230	138	0.7	0-4
24	Kp1	20-40	5630	284	0.5	0-4
24a	Kp1	20-40	250	17	0.8	0-3
24b	Kp1	20-40	700	52	0.8	0-4
24c	Kp1	20-40	750	28	0.4	0-4
24d	Kp1	20-40	1100	53	0.5	0-3
24e	Kp1	20-40	2830	134	0.5	0-4
25	Kcd	10-15	1340	153	1.1	0-5
26	Kcdc	10-15	1160	38	0.3	0-2

TABLE A-3. Summary of Fracture Data for High Angle Fractures

Site	Stratigraphic Unit	Thickness (feet)	Length of Traverse (feet)	Total Fractures	Ave. No. Fractures/10 ft	Range
16	Kp1	20-30	640	19	0.3	0-4
17	Kp1	20-30	670	14	0.2	0-2
18	Kcd	10-15	520	0	---	---
19	Kcd	10-20	640	5	0.1	0-2
20	Kcd	10-25	780	6	0.1	0-1
21	Kg1	30-40	520	19	0.4	0-5
22	Kg1	20-40	1500	3	0.02	0-1
23	Kp1	10-25	230	54	0.3	0-3
24	Kp1	20-40	5630	111	0.2	0-3
24a	Kp1	20-40	250	12	0.5	0-2
24b	Kp1	20-40	700	21	0.3	0-3
24c	Kp1	20-40	750	27	0.4	0-2
24d	Kp1	20-40	1100	15	0.1	0-3
24e	Kp1	20-40	2830	36	0.1	0-3
25	Kcd	10-15	1340	34	0.3	0-6
26	Kcdc	10-15	1160	14	0.2	0-2

TABLE A-4. Summary of Average Fracture Spacing by Stratigraphic Unit

11/11/83

11/11/83

Site	Thickness (feet)	All Fractures	Average Fractures/10 ft	Vertical Fractures	Average Fractures/10 ft	High Angle Fractures	Average Fractures/10 ft
27	10'-20'	120	2.4				
23	10'-25'	192	0.9	138	0.7	54	0.3
16	20'-30'	54	0.9	34	0.6	19	0.3
17	20'-30'	79	1.2	65	1.0	14	0.2
24	20'-40'	395	0.7	284	0.5	111	0.2
24a	20'-40'	29	1.3	17	0.8	12	0.5
24b	20'-40'	73	1.1	52	0.8	21	0.3
24c	20'-40'	55	0.7	28	0.4	27	0.4
24d	20'-40'	68	0.6	53	0.5	15	0.1
24e	20'-40'	170	0.6	134	0.5	36	0.1
29	15'	272	2.8				
25	10'-15'	187	1.4	153	1.1	34	0.3
18	10'-15'	0	---	0	---	0	---
19	10'-20'	13	0.2	8	0.4	5	0.1
28	2'-25'	31	2.1				
20	10'-25'	33	0.4	27	0.4	6	0.1

Kp1

Kcd

TABLE A-4 (Cont'd). Summary of Average Fracture Spacing by Stratigraphic Unit

Site	Thickness (feet)	All Fractures	Average Fractures/10 ft	Vertical Fractures	Average Fractures/10 ft	High Angle Fractures	Average Fractures/10 ft
26	10'-15'	54	0.5	38	0.3	14	0.2
30	10'-30'	122	3.8				
22	20'-40'	111	0.8	108	0.7	3	0.02
21	30'-40'	107	2.1	88	2.1	19	0.4
31	30'-40'	92	1.3				
32	50'-70'	123	1.4				

Kcdc

Kg/Kg1/Kgu

TABLE A-5. Frequency of Occurrence of Fractures Arranged by Lithologic Unit

<u>Site</u>	<u>Number of Fractures</u>										
	<u>0</u>	<u>1</u>	<u>2</u>	<u>3</u>	<u>4</u>	<u>5</u>	<u>6</u>	<u>7</u>	<u>8</u>	<u>9</u>	<u>10</u>
<u>Kp1</u>											
16 (T)	29	23	8	2	1	1					
16 (V)	36	19	5	0	0	1					
16 (H)	51	10	1	1	1						
17 (T)	20	24	16	5	2						
17 (V)	22	25	12								
17 (H)	55	12	1								
23 (T)	77	76	47	6	1						
23 (V)	101	71	26	5							
23 (H)	162	32	8	2							
24 (T)	288	167	86	13	4						
24 (V)	349	149	46	9	4						
24 (H)	456	70	16	3							
24a(T)	6	6	10	1							
24a(V)	11	8	3	1							
24a(H)	14	6	3								
24b(T)	26	23	15	4	2						
24b(V)	37	21	7	3	2						
24b(H)	52	14	2	1							

T = Total Fractures

V = Vertical Fractures

H = High Angle Fractures

TABLE A-5 (Cont'd). Frequency of Occurrence of Fractures Arranged by Lithologic Unit

<u>Site</u>	<u>Number of Fractures</u>										
	<u>0</u>	<u>1</u>	<u>2</u>	<u>3</u>	<u>4</u>	<u>5</u>	<u>6</u>	<u>7</u>	<u>8</u>	<u>9</u>	<u>10</u>
24c(T)	40	18	15	1	1						
24c(V)	56	12	6	0	1						
24c(H)	55	13	7								
24d(T)	59	28	17	2							
24d(V)	67	26	12	1							
24d(H)	85	5	3	1							
24e(T)	157	93	29	5	1						
24e(V)	178	82	18	4	1						
24e(H)	250	32	1	1							
27 (T)	4	14	8	12	7	2		1		1	
<u>Kcd</u>											
18 (T)	52										
18 (V)	52										
18 (H)	52										
19 (T)	52	11	1								
19 (V)	56	8									
19 (H)	60	3	1								
20 (T)	49	25	4								
20 (V)	53	19	4								
20 (H)	72	6									

Table A-5 (Cont'd). Frequency of Occurrence of Fractures Arranged by Lithologic Unit

<u>Site</u>	<u>Number of Fractures</u>										
	0	1	2	3	4	5	6	7	8	9	10
25 (T)	34	47	32	13	4	3	1				
25 (V)	40	47	31	9	3	1					
25 (H)	119	8	2	3	1	1	1				
28 (T)	2	5	1	4	3						
29 (T)	8	24	17	19	3	13	7	3	1	1	
<u>Kcdc</u>											
26 (T)	65	32	11								
26 (V)	73	28	5								
26 (H)	85	8	3								
<u>Kg/Kgu/Kgl</u>											
21 (T)	7	12	21	5	2	4					1
21 (V)	8	13	17	4	1	3					1
21 (H)	44	3	2	1	1	1					
22 (T)	76	48	18	5	3						
22 (V)	77	49	16	5	3						
22 (H)	148	3									
30 (T)	0	2	6	7	5	7	3	2			
31 (T)	19	31	11	6	4	1					
32 (T)	19	29	27	12	1						

# APPENDIX B

## AERIAL PHOTOGRAPH LINEAMENT ANALYSIS

### Discussion

Figures B-1 through B-4 - Rose diagrams, Zones I - III

Tables B-1 through B-3 - Linear counts, Zones I - III

Table B-4 - Summary of primary and secondary aerial photograph linear orientations

## AERIAL PHOTOGRAPH LINEAMENT ANALYSIS

A photomosaic covering an area of four 7½ minute USGS topographic maps was prepared by Intrasearch, Inc. and used as the basemap in this study. The Technology Applications Center of the University of New Mexico (TAC) analyzed this mosaic and low altitude stereographic photography in making a map of linear features (lineaments). These lineaments were plotted on a scale of 1:24,000 and are presented in Plate V. Using photogrametric techniques, TAC defined lineaments ranging in length from 100 to 54,400 feet. Variations in vegetation, trends in stream channels, outcrop patterns, lithologic variations, and fracture patterns were some of the features used to determine these lineaments.

The study area is in a region of semi-arid climatic conditions. The geomorphology of the area is typical of these conditions and the style of weathering lends itself to the enhancement of pre-existing structures (zones of monoclinial flexures, regional and local fracturing and lithologic contrasts).

The basemap was divided into sections as indicated by Map A-1. This particular pattern was used to reflect lineament trends associated with the major structural features of the area (Plate III), and to contrast differing environments of deposition and stress and their surficial expression as lineaments.

The three structurally defined zones were then subdivided according to the type of outcrop analyzed. The first subdivision (Kcc/Kmm) includes the sandy shales and interbedded sandstones of the Crevasse Canyon Formation, subunits of the Mancos Shale, and the Gallup Sandstone. These formations crop out at or near the site area and were investigated for regional trends and distributions near major features.

The second subdivision (Kpl/Kmfc) is the approximate outcrop area of the Point Lookout Sandstone and Cleary Coal Member (?) of the Menefee Formation. These units are stratigraphically higher than the Kcc/Kmm group and surface exposures are characteristic of thick sandstones.

The lineaments (Plate V) were grouped by orientation and unweighted length. Rose diagrams were generated for all lineaments in each subzone (Figs. B-1 - B-4). Rose diagrams contrasting lineaments greater than and less than 1000 feet are also presented. The data used in preparing the rose diagrams are presented in Tables B-1 - B-4. A summary of the rose diagrams is given in Table B-4.

The pi diagram data correlate well with the rose diagram data. This comparison indicates paralleling regional orthogonal trends in both lineaments and fractures. The fracture count data show an increase in the number of fractures per 100 feet of traverse as major lineaments are crossed. The site occupies the intersection area of three strong lineaments - the Pipeline Canyon, Fort Wingate and a "composite" trend to the north (see page 17). From the strong geomorphic expression, structural geology, and fracture data the lineaments above should be considered as potential areas of higher conductivity than surrounding areas.

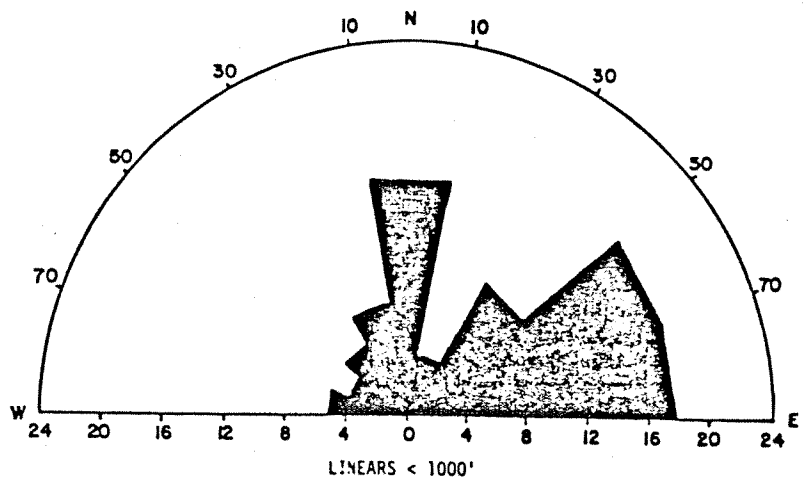
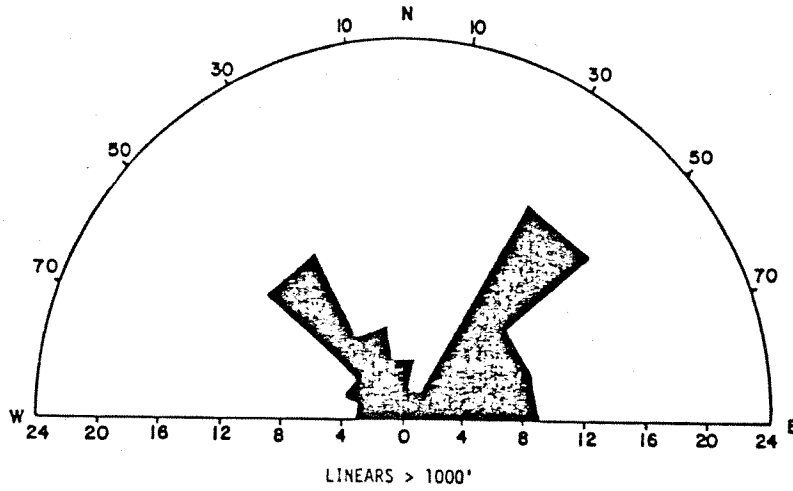
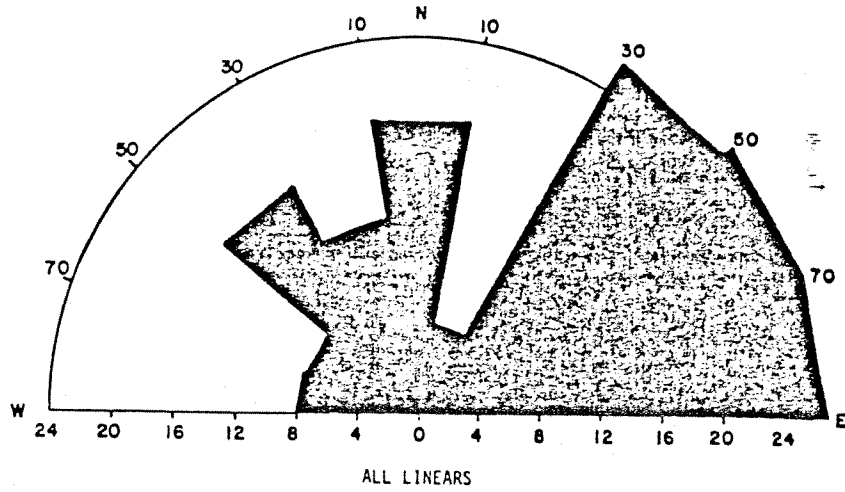


Figure B-1. Rose diagrams for aerial photograph linears in the Crevasse Canyon Formation outcrop area.

ZONE I

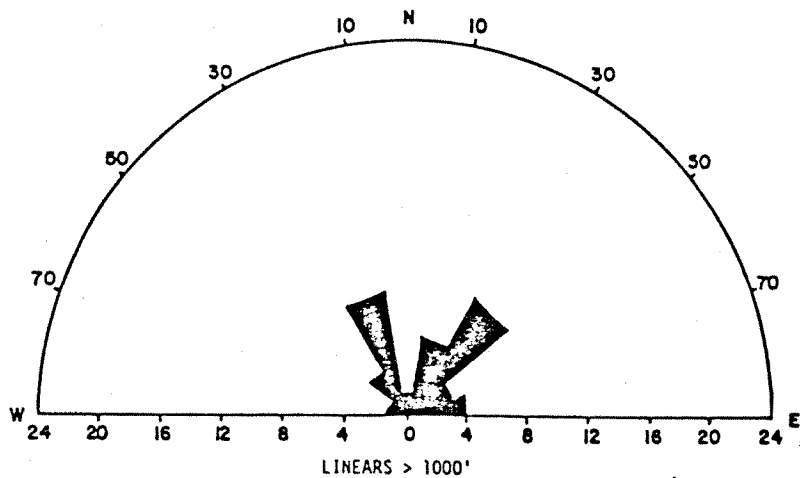
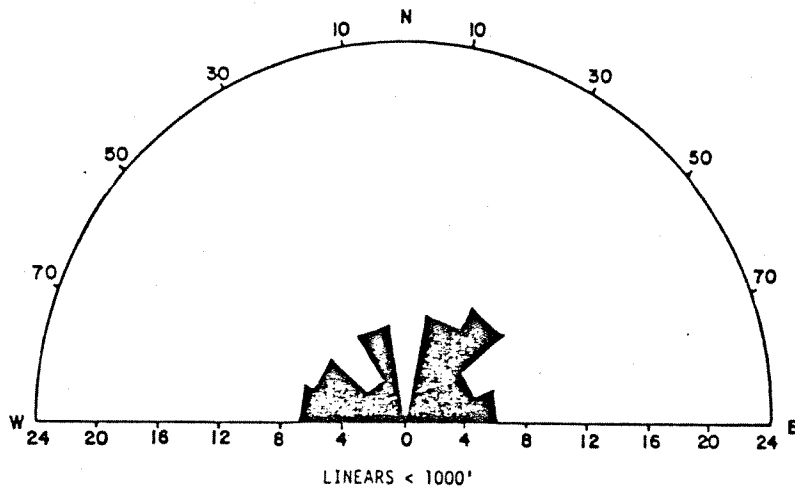
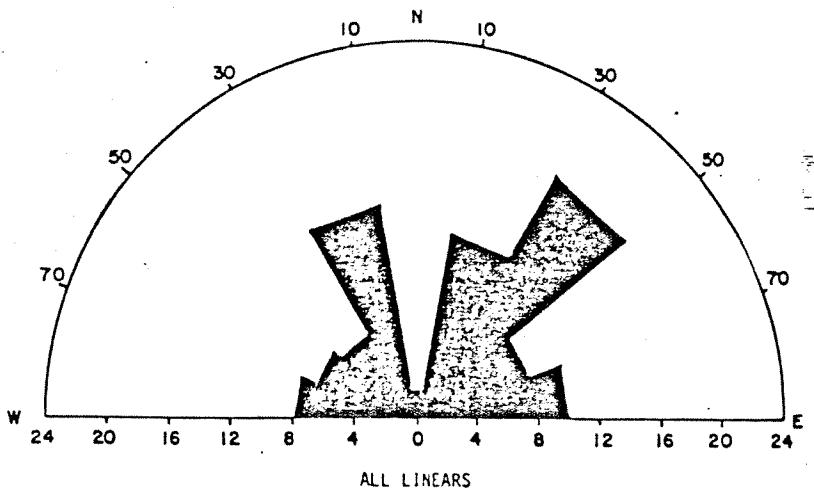


Figure B-2. Rose diagrams for aerial photograph linears in the Crevasse Canyon Formation outcrop area.

ZONE II

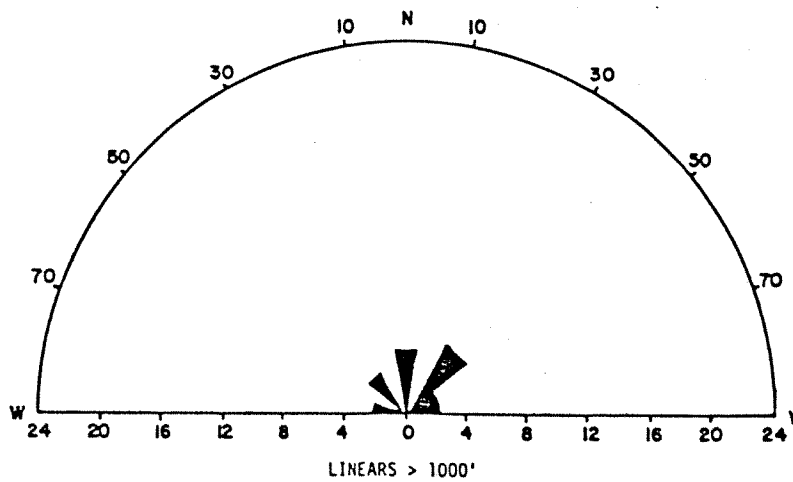
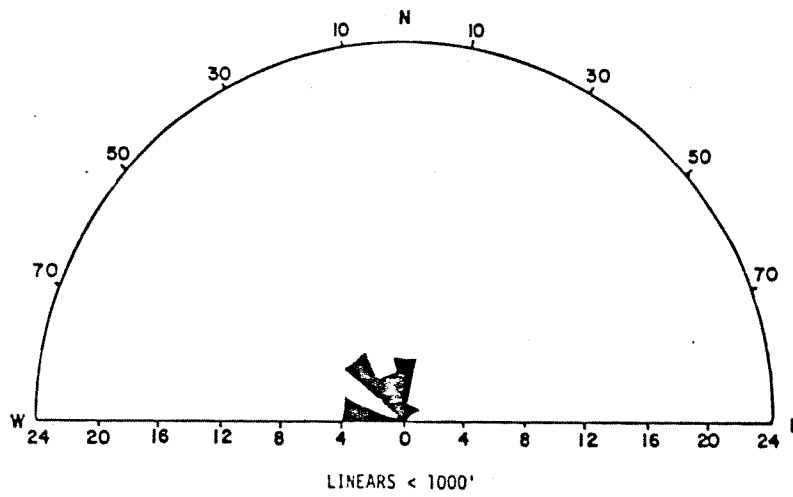
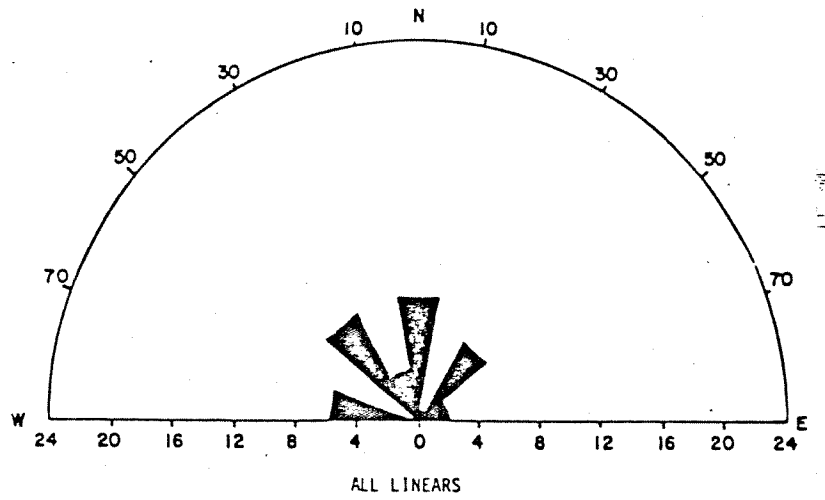


Figure B-3. Rose diagrams for aerial photograph linears in the Crevasse Canyon Formation outcrop area.

ZONE III

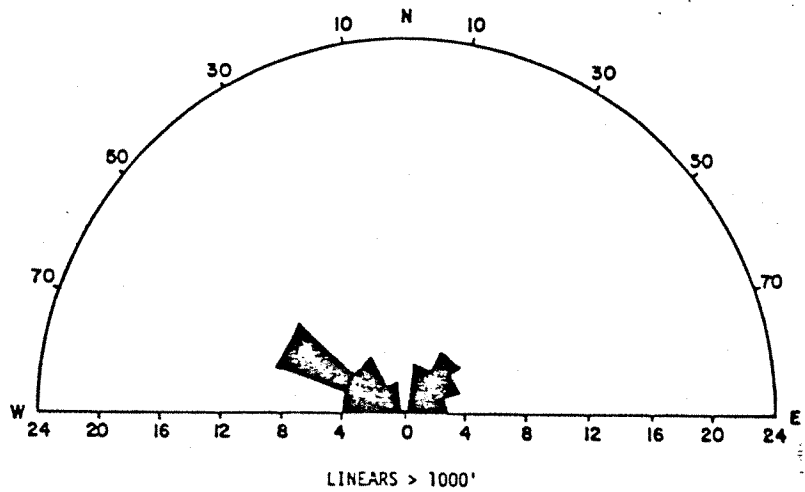
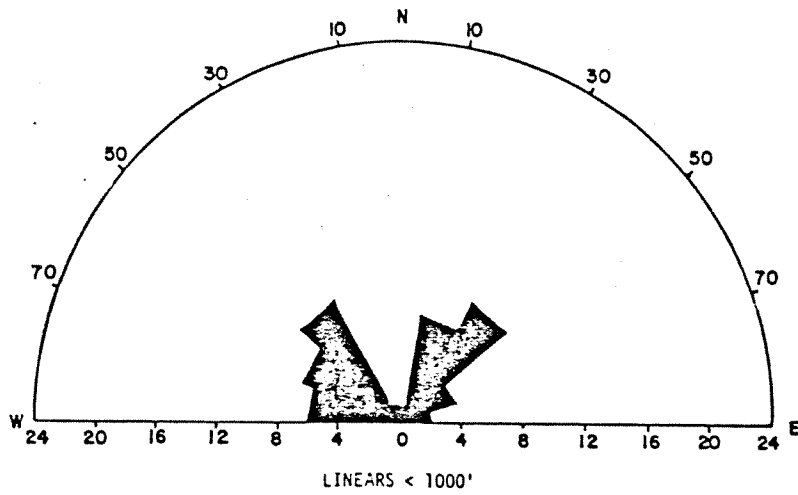
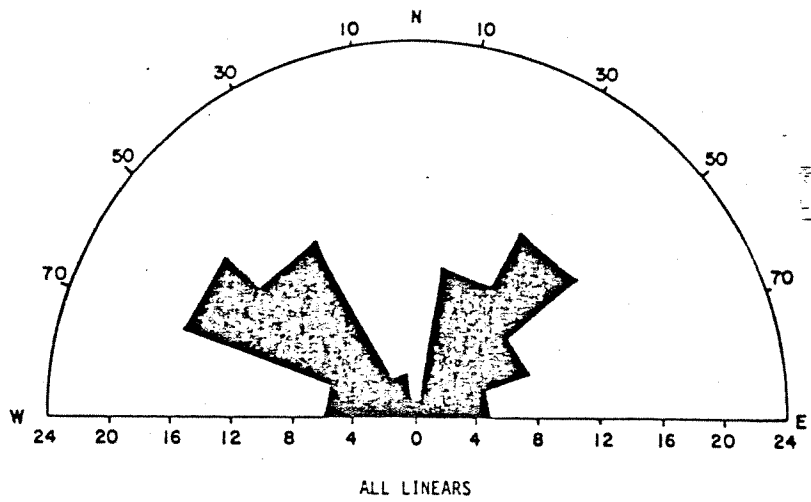


Figure B-4. Rose diagrams for aerial photograph linears in the Crevasse Canyon Formation outcrop area.

ZONE IV

TABLE B-1. Linear Count

ZONE I

Linear Length (feet) Orientation	0 to 500'	500' to 1000'	1000' to 2000'	2000' to 3000'	3000' to 4000'	74000'
<u>Kcc/Kmm</u>						
EW - N70W	1	4	1	2	0	0
N70W - N50W	0	4	3	0	0	1
N50W - N30W	1	4	7	3	1	1
N30W - N10W	4	3	4	1	1	0
N10W - N10E	8	7	4	0	0	0
N10E - N30E	3	1	2	0	0	0
N30E - N50E	3	7	10	3	1	2
N50E - N70E	9	9	7	0	1	0
N70E - EW	9	9	7	1	1	0
<u>Kpl/Kmfc</u>						
EW - N70W	3	3	2	0	2	0
N70W - N50W	2	5	8	0	0	1
N50W - N30W	2	7	2	2	0	0
N30W - N10W	0	1	1	0	0	1
N10W - N10E	1	0	0	0	0	0
N10E - N30E	3	4	1	1	1	0
N30E - N50E	1	8	4	0	0	1
N50E - N70E	1	3	3	1	0	0
N70E - EW	0	2	0	1	1	1

TABLE B-2. Linear Count

ZONE II

Linear Length (feet) Orientation	0 to 500'	500' to 1000'	1000' to 2000'	2000' to 3000'	3000' to 4000'	74000'
<u>Kcc/Kmm</u>						
W - 70W	4	3	1	0	0	0
70W - 50W	1	5	1	0	0	0
50W - 30W	0	3	3	0	0	0
30W - 10W	4	2	6	2	0	0
10W - 10E	0	0	0	1	0	0
10E - 30E	3	4	4	1	0	0
30E - 50E	4	5	4	1	2	2
50E - 70E	2	3	3	0	0	0
70E - E	5	1	4	0	0	0

TABLE E-3. Linear Count

ZONE III

Linear Length (feet) Orientation	0 to 500'	500' to 1000'	1000' to 2000'	2000' to 3000'	3000' to 4000'	74000
<u>Kcc/Kmm</u>						
W - 70W	1	3	2	0	0	0
70W - 50W	0	0	0	0	0	0
50W - 30W	3	2	2	0	1	0
30W - 10W	0	3	0	0	0	0
10W - 10E	0	4	3	1	0	0
10E - 30E	0	1	0	0	0	0
30E - 50E	1	0	3	1	0	1
50E - 70E	0	0	2	0	0	0
70E - E	0	0	2	2	0	0

TABLE B-4. Summary of Primary and Secondary Aerial Photograph Linear Orientations

<u>Area &amp; Fracture Length</u>	<u>Primary</u>	<u>Orientation</u>	<u>Secondary</u>
<b>1. Zone I</b>			
<u>Kcc/Kmm</u>			
>1000'	N50 - 55E		N35W
<1000'	N70E		N10 - 15W
All	N65E		N30W
-----			
<u>Kpl/Kmfc</u>			
>1000'	N60W		N45E
<1000'	N50W		N40E
All	N40W		N65E
<hr/>			
<b>2. Zone II</b>			
<u>Kcc/Kmm</u>			
>1000'	N40E		N30W
<1000'	N40E		N60W
All	N40E		N30W
<hr/>			
<b>3. Zone III</b>			
<u>Kcc/Kmm</u>			
>1000'*	N50E		N30W
<1000'	N40W		N10W
All	No Preferred Orientation		

\* These linears show a bimodal distribution as indicated but neither orientation is preferred.

REFERENCES CITED

## REFERENCES CITED

- Beaumont, E. C., 1971, Stratigraphic distribution of coal in San Juan Basin: New Mex. Bur. Mines and Min. Res. Mem. 25, p. 15-30.
- Belousov, V. V., 1962, Basic problems in geotectonics: New York, McGraw-Hill Book Co., Inc., p. 816.
- Bonilla, M. G., 1967, Historic surface faulting in continental United States and adjacent parts of New Mexico; USGS open-file report.
- Coney, P. J., 1976, Plate tectonics and the Laramide orogeny: New Mex. Geol. Soc., Spec. Pub. no. 6, p. 5-10.
- Couples, G. and Stearns, D. W., 1978, Analytical solutions applied to structures of the Rocky Mountain foreland on local and regional scale, in Matthews, V., III, ed., Laramide folding associated with basement block faulting in the western United States: Geol. Soc. Amer. Mem. 151, p. 313-336.
- Edmonds, R. J., 1961, Geology of the Nutria monocline, New Mexico: unpublished master's thesis, Univ. of New Mexico, p. 100.
- Gibbons, J. F., III, 1962, Shear and tension fracture patterns in northwest and northcentral Arkansas: unpublished master's thesis, Univ. of Arkansas, p. 70.
- 1971, Tectonics of the eastern Ozarks: unpublished Ph.D. dissertation, Syracuse University, p. 75.
- 1979, A groundwater discharge plan using below grade tailings disposal Marquez Mill, N.M.: unpublished report, Science Applications, Inc.
- and Ferrell, C. C., 1980, Fracture model for the Waste Isolation Pilot Program: in press, Sandia report.
- Harris, S. F., Taylor, G. L., and Walper, J. J., 1960, Relation of deformational fractures in sedimentary rocks to regional and local structure: Am. Assoc. Petroleum Geologists Bull., v. 44, p. 1853-1873.
- Handin, J., Hager, R. V., Jr., Friedman, M., and Feather, J. N., 1963, Experimental deformation of sedimentary rocks under confining pressure: Pore pressure tests: Am. Assoc. Petroleum Geologists Bull., v. 47, p. 717-755.
- Hobbs, D. W., 1967, Formation of tension joints: Geol. Mag., v. 104, p. 550-556.
- Kirk, A. R. and Zech, R. S., 1977, The transgressive and regressive relationships between the Upper Cretaceous Mulatto Tongue of the Mancos Shale and the Dalton Sandstone Member of the Crevasse Canyon Formation, Gallup-Pinedale area, New Mexico: New Mex. Geol. Soc. Guidebook, 28th Field Conf., San Juan Basin III, p. 185-192.

- Newton, C. A., Cash, D. J., Olsen, K. H. and Homuth, E. F., 1976, Los Alamos scientific programs in the vicinity of Los Alamos, New Mexico: LASL report no. LA-6406-MS, p. 42.
- McGuire, Robin K., 1977, Effects of uncertainty in seismicity on estimates of seismic hazard for the east coast of the U.S.: Bull. Seis. Soc. Am., v. 67, p. 827-848.
- Molenaar, C. M., 1973, Sedimentary facies and correlation of the Gallup Sandstone and associated formations, northwestern New Mexico, *in* Fassett, J. E., ed., Cretaceous and Tertiary rocks of the southern Colorado plateau: Four corners Geol. Soc. Mem., p. 85-110.
- 1977a, Stratigraphy and depositional history of Upper Cretaceous rocks of the San Juan Basin area, New Mexico and Colorado, with a note on economic resources: New Mex. Geol. Soc. Guidebook, 28th Field Conf., San Juan Basin III, p. 159-166.
- 1977b, The Pinedale oil seep--an exhumed stratigraphic trap in the southwestern San Juan Basin: New Mex. Geol. Soc. Guidebook, 28th Field Conf., San Juan Basin III, p. 159-166.
- O'Neill, Kevin, 1977, The transient three dimensional transport of liquid and heat in fractured porous media: unpublished Ph.D. dissertation, Princeton University, p. 600.
- Price, N. J., 1959, Mechanics of jointing: Geol. Mag., v. 96, p. 149-167.
- 1966, Fault and joint development in brittle rock: London, Pergamon Press, p. 176.
- Prucha, J. J., Graham, J. A., and Nickelsen, R. P., 1965, Basement controlled deformation in Wyoming province of Rocky Mountains foreland: Am. Assoc. Petrol. Geol. Bull., v. 49, no. 7, p. 792-966.
- Robinson, L. H., Jr., 1959, The effect of pore and confining pressure on the failure process in sedimentary rock: Colorado School Mines Quart. 54, no. 3, p. 177-199.
- Sanford, A. R., 1959, Analytical and experimental study of simple geologic structures: Geol. Soc. Amer. Bull., v. 76, p. 19.
- Budding, A. J., Hoffman, J. P., Alptekin, O. S., Rush, C. A., and Topozada, T. R., 1972, Seismicity of the Rio Grande rift in New Mexico: New Mexico State Bur. Mines Min. Res., Circ. 120, p. 1-19.
- Sanford, S., Caravella, F. J., Merritt, L., Sheldon, J., and Ward, R.M., 1978, A report on seismic studies of the Los Medanos area in southeastern New Mexico: New Mexico Institute of Mining and Technology, report to Sandia Labs, contract no. 03-6233.

- Secor, D. T., Jr., 1968, Mechanics of natural extension fracture, *in* Baer, A. J. and Norris, D. K., eds., Conference on tectonics: Canada Geol. Survey paper 68-52, p. 79-95.
- Smith, R. B. and Sbar, M. L., 1974, Contemporary tectonics and seismicity of the western United States with emphasis on the intermountain seismic belt: Geol. Soc. Am. Bull., v. 85, p. 1205-1218.
- Sowers, G. M., 1973, Theory of spacing of extension fracture, *in* Pincus, H., ed., Geological factors in rapid excavation: Geol. Soc. Amer. Engineering Geology, Case history No. 9, p. 27-53.
- Stearns, D. W., 1968, Certain aspects of fracture in naturally deformed rocks, *in* Recker, R. E., ed., NSF advanced science seminar in rock mechanics for college teachers of structural geology: Bedford, Air Force Cambridge Research Labs, p. 97-116.
- Woodward, L. A., 1976, Laramide deformation of Rocky Mountain Foreland: geometry and mechanics: New Mexico Geol. Soc. Spec. Pub., No. 6, p. 5-10.
- and Callender, B. J. F., 1977, Tectonic framework of the San Juan Basin: New Mex. Geol. Soc. Guidebook, 28th Field Conf., San Juan Basin III, p. 209-212.
- Zoback, M. L. and Zoback, M., 1980, Interpretative stress map of the conterminous United States: unpublished manuscript, USGS.

00000000

0000

00000000

00000000